

AD-A089 443

NAVAL OCEAN SYSTEMS CENTER SAN DIEGO CA
IMPLEMENTATION AND EVALUATION OF THE DISTURBANCE AMPLIFICATION --ETC(U)
MAR 80 T S MAUTNER
NOSC/TD-340

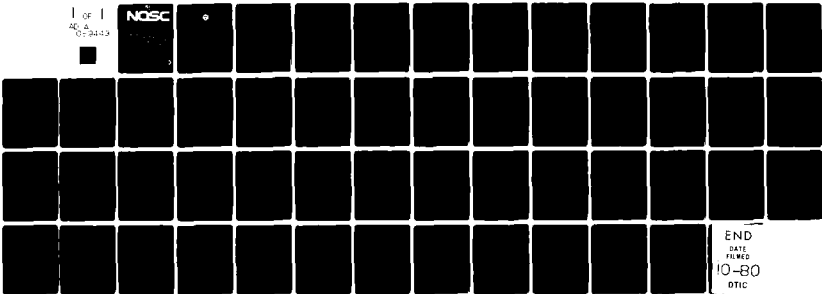
F/G 20/4

ML

UNCLASSIFIED

1 of 1
40-24430
[Redacted]

NOSC



END
DATE
FILED
10-80
OTIC

LEVEL # *12*
NOSC

NOSC TD 340

AD A 089443

NOSC TD 340

Technical Document 340

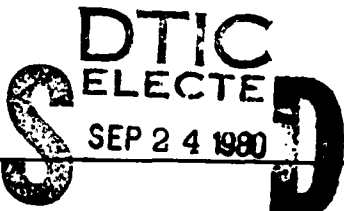
**IMPLEMENTATION AND EVALUATION
OF THE DISTURBANCE AMPLIFICATION
IN BOUNDARY LAYERS (DABL)
COMPUTER PROGRAM:
A USER'S MANUAL**

T. S. Mautner

March 1980

Prepared for
Naval Sea Systems Command

Approved for public release; distribution unlimited



A

NAVAL OCEAN SYSTEMS CENTER
SAN DIEGO, CALIFORNIA 92152

DDC FILE COPY
80 9 24 019



NAVAL OCEAN SYSTEMS CENTER, SAN DIEGO, CA 92152

AN ACTIVITY OF THE NAVAL MATERIAL COMMAND

SL GUILLE, CAPT, USN

Commander

HL BLOOD

Technical Director

ADMINISTRATIVE INFORMATION

The work reported herein was performed as a portion of the research conducted at NOSC within the Torpedo Hydrodynamics and Hydroacoustics Program funded by the Naval Sea Systems Command (NAVSEA 63R31), Dr. T. E. Peirce, Program Manager. The work was performed in the Fluid Mechanics Branch (Code 6342), Hydromechanics Division of the Fleet Engineering Department.

Released by
J. H. Green, Head
Hydromechanics Division

Under authority of
R. H. Hearn, Head
Fleet Engineering Department

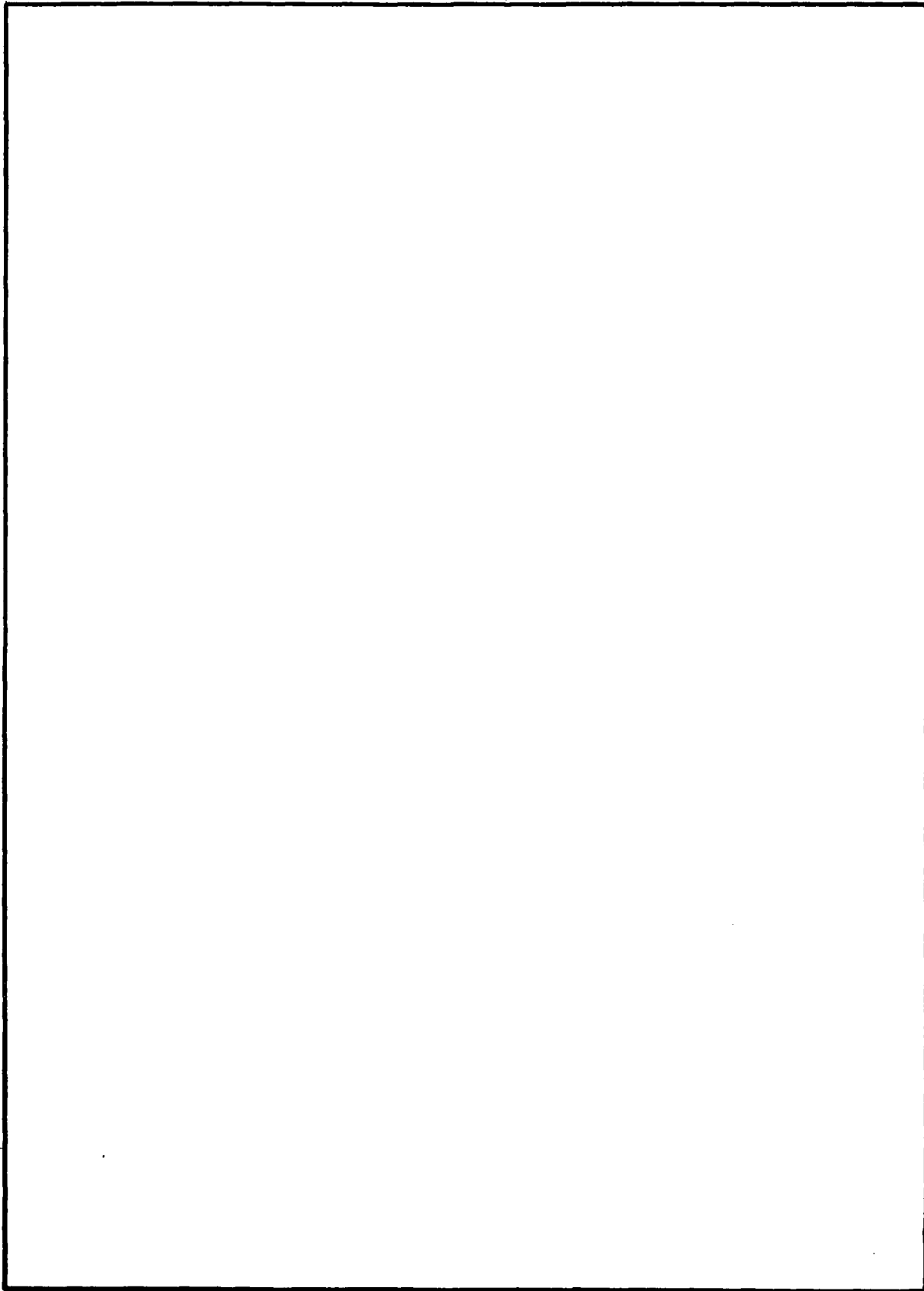
UNCLASSIFIED

SECURITY CLASSIFICATION OF THIS PAGE (When Data Entered)

REPORT DOCUMENTATION PAGE		READ INSTRUCTIONS BEFORE COMPLETING FORM
1. REPORT NUMBER TD 340	2. GOVT ACCESSION NO. AD-AC89443	3. RECIPIENT'S CATALOG NUMBER
4. TITLE (and Subtitle) IMPLEMENTATION AND EVALUATION OF THE DISTURBANCE AMPLIFICATION IN BOUNDARY LAYERS (DABL) COMPUTER PROGRAM: A USER'S MANUAL		5. TYPE OF REPORT & PERIOD COVERED Research
7. AUTHOR(s) T. S. Mautner		6. PERFORMING ORG. REPORT NUMBER
9. PERFORMING ORGANIZATION NAME AND ADDRESS Naval Ocean Systems Center San Diego, CA 92152		10. PROGRAM ELEMENT, PROJECT, TASK AREA & WORK UNIT NUMBERS
11. CONTROLLING OFFICE NAME AND ADDRESS		12. REPORT DATE March 1980
14. MONITORING AGENCY NAME & ADDRESS (if different from Controlling Office)		13. NUMBER OF PAGES 50
16. DISTRIBUTION STATEMENT (of this Report) Approved for public release; distribution unlimited		15. SECURITY CLASS. (of this report) Unclassified
17. DISTRIBUTION STATEMENT (of the abstract entered in Block 20, if different from Report)		
18. SUPPLEMENTARY NOTES		
19. KEY WORDS (Continue on reverse side if necessary and identify by block number) DABL TAPS Disturbance amplification		
20. ABSTRACT (Continue on reverse side if necessary and identify by block number) This report describes the implementation and evaluation of the Fortran IV computer program DABL (Disturbance Amplification in Boundary Layers) which calculates the growth of small disturbances in laminar boundary layers.		

UNCLASSIFIED

SECURITY CLASSIFICATION OF THIS PAGE (When Data Entered)



UNCLASSIFIED

SECURITY CLASSIFICATION OF THIS PAGE(When Data Entered)

CONTENTS

DEFINITION OF TERMS ... page 3

INTRODUCTION ... 5

TWO-DIMENSIONAL GEOMETRY ... 6

AXISYMMETRIC GEOMETRY ... 12

COMPUTER PROGRAM USAGE ... 23

 Definition of the Input Variables ... 23

 Method of Inputting Data Tables ... 25

 Program Input Scheme ... 26

COMPUTER PRINTOUT ... 29

 Included Items ... 29

 Printout Definitions ... 29

SUMMARY ... 32

REFERENCES ... 33

APPENDIX A: Computer Listing – Heated Flat Plate ... 34

APPENDIX B: Computer Listing – Heated 9:1 Ellipsoid ... 42

Accession For	
NTIS	General
DBI	14B
Unrestricted	
Justification	
By _____	
Distribution	
Approved by _____	
Avail.	Available or Specified
Dist.	A

ILLUSTRATIONS

1. Comparison of the neutral stability curves of a flat plate . . . page 7
2. Comparison of the disturbance amplification ratios of a flat plate . . . 9
3. Comparison of the neutral stability points of a flat plate with 2.78°C surface overheat . . . 11
4. Potential flow velocity distribution of a 9:1 ellipsoid . . . 13
5. Skin friction coefficient of a 9:1 ellipsoid — $R_L \cong 4.5 \times 10^6/\text{ft}$. . . 13
6. Boundary layer shape factor of a 9:1 ellipsoid — $R_L \cong 4.5 \times 10^6/\text{ft}$. . . 14
7. Displacement thickness Reynolds number of a 9:1 ellipsoid — $R_L \cong 4.5 \times 10^6/\text{ft}$. . . 14
8. Computed growth rates of a 9:1 ellipsoid for $\omega_f = 0.486 \times 10^{-4}$ —
 $R_L \cong 4.5 \times 10^6/\text{ft}$. . . 15
9. Computed growth rates of a 9:1 ellipsoid for $\omega_f = 0.32 \times 10^{-4}$ —
 $R_L \cong 4.5 \times 10^6/\text{ft}$. . . 16
10. Comparison of the computed amplification ratios of a 9:1 ellipsoid for
 $\omega_f = 0.486 \times 10^{-4}$ and $\omega_f = 0.32 \times 10^{-4}$ — $R_L \cong 4.5 \times 10^6/\text{ft}$. . . 17
11. Surface temperature distribution of a 9:1 ellipsoid — $R_L \cong 4.49 \times 10^6/\text{ft}$. . . 18
12. Skin friction coefficient of a heated 9:1 ellipsoid — $R_L \cong 4.49 \times 10^6/\text{ft}$. . . 18
13. Boundary layer shape factor of a heated 9:1 ellipsoid — $R_L \cong 4.49 \times 10^6/\text{ft}$. . . 18
14. Displacement thickness Reynolds number of a heated 9:1 ellipsoid —
 $R_L \cong 4.49 \times 10^6/\text{ft}$. . . 19
15. Computed growth rates of a heated 9:1 ellipsoid for $\omega_f = 0.32 \times 10^{-4}$ —
 $R_L \cong 4.49 \times 10^6/\text{ft}$. . . 20
16. Computed growth rates of a heated 9:1 ellipsoid for $\omega_f = 0.18 \times 10^{-4}$ —
 $R_L \cong 4.49 \times 10^6/\text{ft}$. . . 21
17. Comparison of the computed amplification ratios of a heated 9:1 ellipsoid —
 $R_L \cong 4.49 \times 10^6/\text{ft}$. . . 22
18. Input direction for the axisymmetric body coordinates . . . 27
19. Input direction for the two-dimensional body coordinates . . . 28

TABLES

1. Summary of the computed values for the neutral curve of an unheated flat plate . . . 8
2. Summary of the computed values for the neutral curve of a heated flat plate ($\Delta T = 2.78^{\circ}\text{C}$) . . . 10

DEFINITION OF TERMS

A/A_0	Disturbance Amplification Ratio
C_f	Skin Friction Coefficient
e^N	The Amplification Ratio ($= A/A_0$) according to linear stability theory
f	Disturbance Frequency - Hz
H	Boundary Layer Shape Factor
L	Reference Length
R_L	Reynolds Number = $U_\infty L/\nu_\infty$
R_{δ^*}	Displacement Thickness Reynolds Number = $U_\infty \delta^*/\nu_\infty$
T	Temperature
U_∞	Free Stream Velocity
$-\alpha_i^*$	Local Relative Growth Rate of a Disturbance
δ^*	Displacement Thickness
ν_∞	Free Stream Kinematic Viscosity
ω_f	Nondimensional Disturbance Frequency = $2\pi f \nu_\infty / U_\infty^2$

INTRODUCTION

This report describes the implementation and evaluation of the Fortran IV computer program DABL (Disturbance Amplification in Boundary Layers – developed at the David Taylor Naval Ship Research and Development Center (DTNSRDC) by vonKerczek and Groves, 1978) which calculates the growth of small disturbances in laminar boundary layers. DABL calculates the amplification ratios, A/A_0 , for heated or unheated, two-dimensional or axisymmetric, incompressible laminar boundary layers. The boundary layer is assumed to be steady and has constant density with the fluid viscosity varying with temperature. The DABL code requires only the body coordinates, surface temperature distribution and body Reynolds number to compute the spatial amplification ratios as a function of arc length and nondimensional disturbance frequency using parallel, viscous flow, linear stability theory. The resulting amplification ratio distribution can be used to locate boundary layer transition via the e^N method.

This report makes no attempt to discuss or evaluate the theoretical and numerical methods used by DABL in computing the boundary layer properties and in performing the boundary layer stability analysis. vonKerczek and Groves (1978) discussed these topics in detail. However, this report does present several examples used to evaluate DABL as modified by the author and adapted to the NOSC UNIVAC 1110 Computer.

Upon receipt of the DABL Program from DTNSRDC, the computer code was altered (to be compatible with UNIVAC 1110) and compiled in ASCII Fortran utilizing a segmented execution mode to conform to the 65K storage limit of the NOSC system. Prior to any further changes, DABL was checked for proper execution using the examples of vonKerczek and Groves (1978).

After the DABL code was operating properly, the following additions/changes were incorporated into the code:

1. The program output was expanded to include both the original and normalized body coordinates and, in the case of heated bodies, the surface temperature distribution.
2. The option to read and write the boundary layer data to mass storage was added.
3. The fluid property definitions were expanded to include air, as well as water, boundary layers.
4. Options were included to allow the stability calculations to proceed regardless of the calculated amplification ratio value and to begin the stability automatic start routine at a prescribed body location.
5. The step function surface temperature distribution was changed to allow the distribution to end prior to the end of the body.

The remainder of the report is divided into several sections. First, DABL was used to compute the neutral stability points for an unheated and heated flat plate and the amplification ratios at several disturbance frequencies for the unheated plate. These results are compared with theory and experiment. Next, a comparison is made between the values of skin friction, shape factor, growth rates and amplification ratios computed by DABL and TAPS (Transition Analysis Program System) for both a heated and unheated 9:1 ellipsoid.

Thirdly, a complete description of the input/output variables and program input scheme of DABL is presented. Finally, abbreviated listings of the computer output for the heated flat plate and the heated 9:1 ellipsoid are included as examples.

Although many of the descriptions found in the original DABL report (vonKerczek and Groves, 1978) are repeated here, the input format for the NOSC version of DABL has been changed completely. Anyone desiring to use this program should contact the author and a listing, card deck or tape and check solutions will be provided.

TWO-DIMENSIONAL GEOMETRY

To evaluate the two-dimensional option of the DABL code, a flat plate geometry was chosen. The test plate is 0.25 inches thick and has a sharp leading edge with a 1.8 degree half angle. There is good agreement with the potential flow velocities computed by DABL and the Douglas Two-Dimensional Cascade Potential Flow Program (Giesing, 1964). The plate has a nearly zero pressure gradient at a zero angle of attack. Overall plate lengths of one and 12 feet were used in the analysis. The coordinates of the one-foot plate and the potential flow velocities are given in Appendix A.

The neutral stability curves for both an unheated plate and a heated plate with a constant surface overheat of 2.78°C were calculated using the automatic starting option of DABL. For each plate length and Reynolds number, R_L/ft , the neutral stability points (where $-\alpha^* = 0$) were located and the corresponding displacement thickness Reynolds number and nondimensional frequency were tabulated and plotted.

Figure 1 compares the neutral stability points computed by DABL (also found in Table 1) with the experimental results of Schubauer and Skramstad (1948) and the theoretical results presented by Ross et al (1970). As the R_L/ft was increased, DABL's automatic starting method calculated nondimensional frequencies ω_f which resulted in neutral points falling within the neutral curve of Ross et al. However, if for a particular R_L/ft , the starting ω_f is decreased, the DABL calculated neutral points fall closer to theoretical and experimental values.

In Figure 2, a comparison is made between the amplification ratios A/A_0 computed by DABL and the theoretical curves of Jordinson (1970) and the experimental data presented by Ross et al (1970). Agreement is good within the common regions of comparison. The additional amplification ratios for $R_L/\text{ft} = 2.0 \times 10^6$ and 5.0×10^6 have been included as further demonstration of DABL's results; however, no comparisons are made.

Finally, the neutral stability points for a heated plate (constant $\Delta T = 2.78^{\circ}\text{C}$) were calculated using DABL (also found in Table 2) and are compared to the experimental results of Strazisar (1976) in Figure 3. As in the unheated case, DABL's automatic starting mode computes frequencies ω_f which result in neutral points falling within the neutral zone defined by Strazisar. In general, DABL produces conservative estimates for the onset of disturbance amplification.

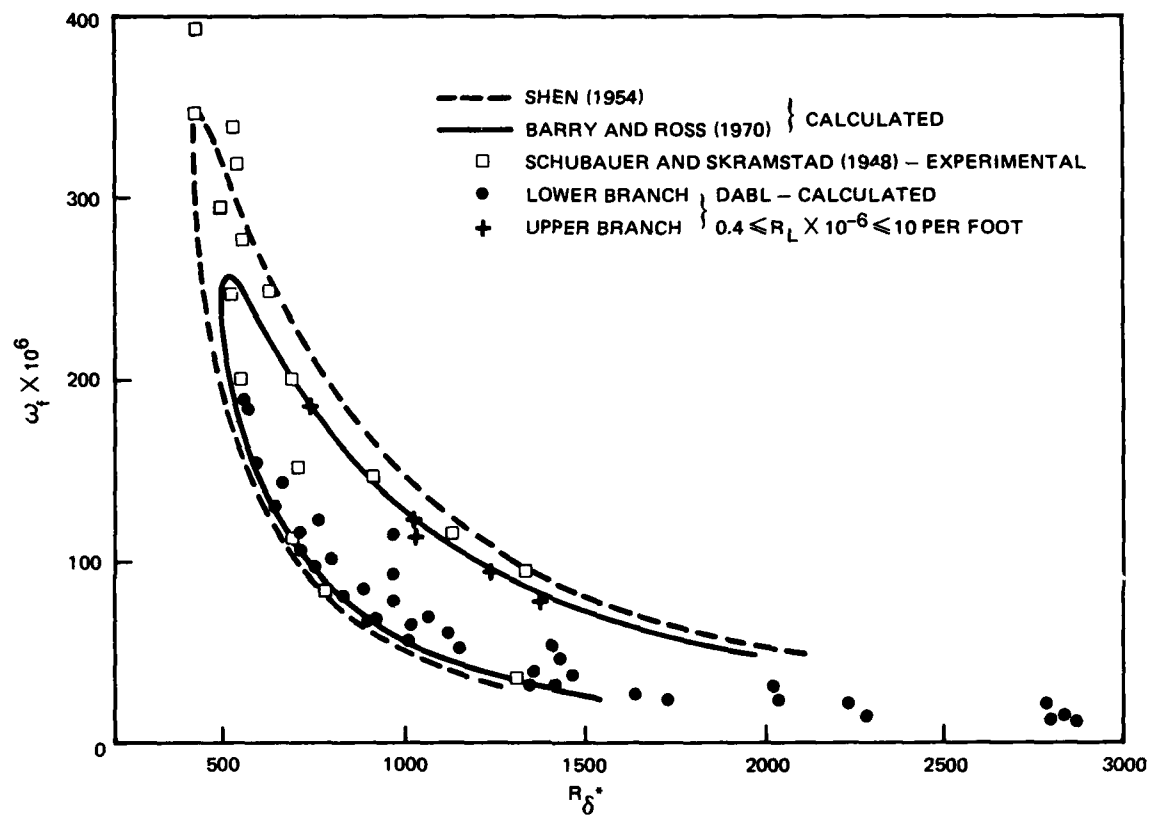


Figure 1. Comparison of the neutral stability curves of a flat plate.

Plate Length, ft	$R_L \times 10^{-6}/\text{ft}$	$\omega_f \times 10^6$	R_δ^*	Fluid
1.00	0.40	189.56	558	Water
		157.34	596	
		130.59	645	
		108.39	704	
	0.50	185.54	570	
		154.00	605	
		127.82	655	
		106.09	712	
		88.06	782	
	1.00	143.57	662	
		119.16	700	
		98.90	753	
		82.09	824	
		68.13	902	
	2.00	122.42	755	
		101.60	794	
		84.33	880	
		70.00	935	
		58.10	1005	
	5.00	113.96	970	
		94.59	962	
		78.51	970	
		65.16	1015	
		54.08	1150	
	10.00	41.00	1360	
		34.00	1420	
		28.00	1640	
		23.50	1730	
12.0	2.00	56.54	1410	
		46.93	1430	
		38.95	1465	
	5.00	30.87	2015	
		25.63	2045	
		21.27	2215	
		17.65	2285	
	10.00	21.36	2780	
		20.09	2770	
		17.73	2800	
		16.68	2820	
		13.84	2870	5085

Table 1. Summary of the computed values for the neutral curve of an unheated flat plate.

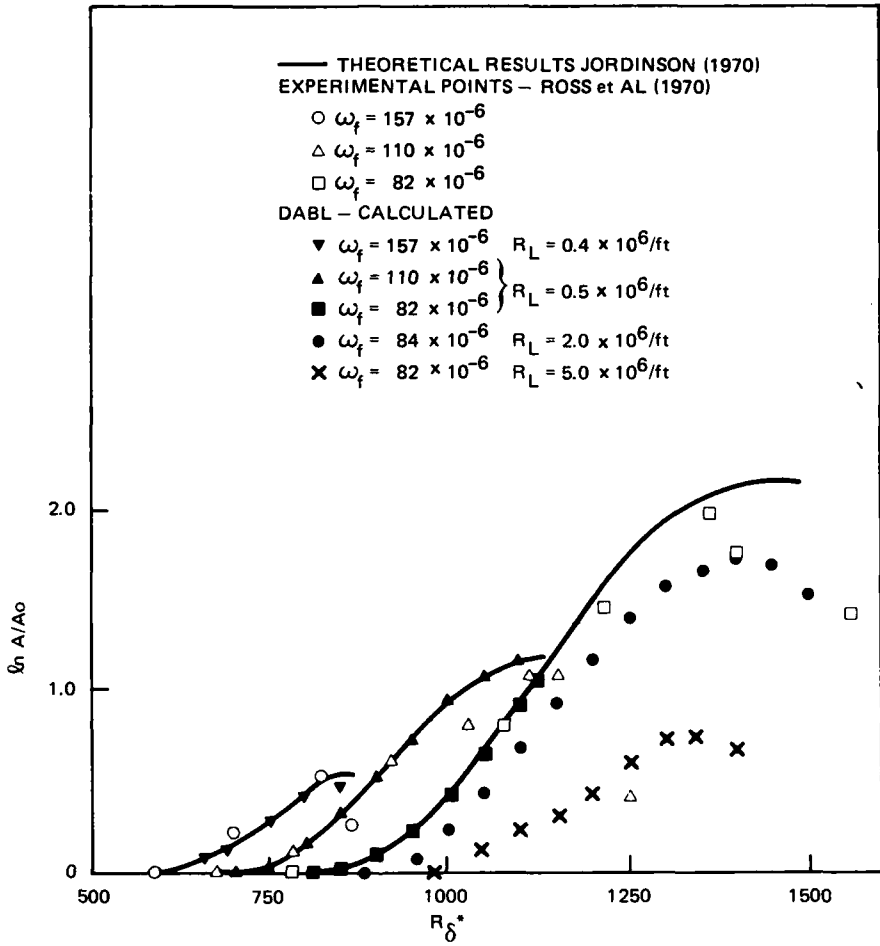


Figure 2. Comparison of the disturbance amplification ratios of a flat plate.

Plate Length, ft	$R_L \times 10^{-6}/\text{ft}$	$\omega_f \times 10^6$	R_δ^*	Fluid
1.00	0.25	173.43	595	Water
	0.50	163.72	615	
		135.89	655	
	1.00	139.30	675	
		115.62	724	
		95.96	780	
		79.65	845	
		66.11	930	
2.00	2.00	118.62	762	785
		118.62	855	1020
		98.46	864	1195
		81.72	890	
		67.83	948	
		56.30	1028	
5.00	5.00	93.70	945	1042
		93.70	1137	1208
		77.77	965	1310
		64.55	1100	1642
		53.57	1137	
5.00	5.00	114.85	800	830
		114.85	980	1040
		95.33	960	1245
		79.12	980	
		65.67	1022	
		54.51	1026	

Table 2. Summary of the computed values for the neutral curve
of a heated flat plate ($\Delta T = 2.78^\circ\text{C}$).

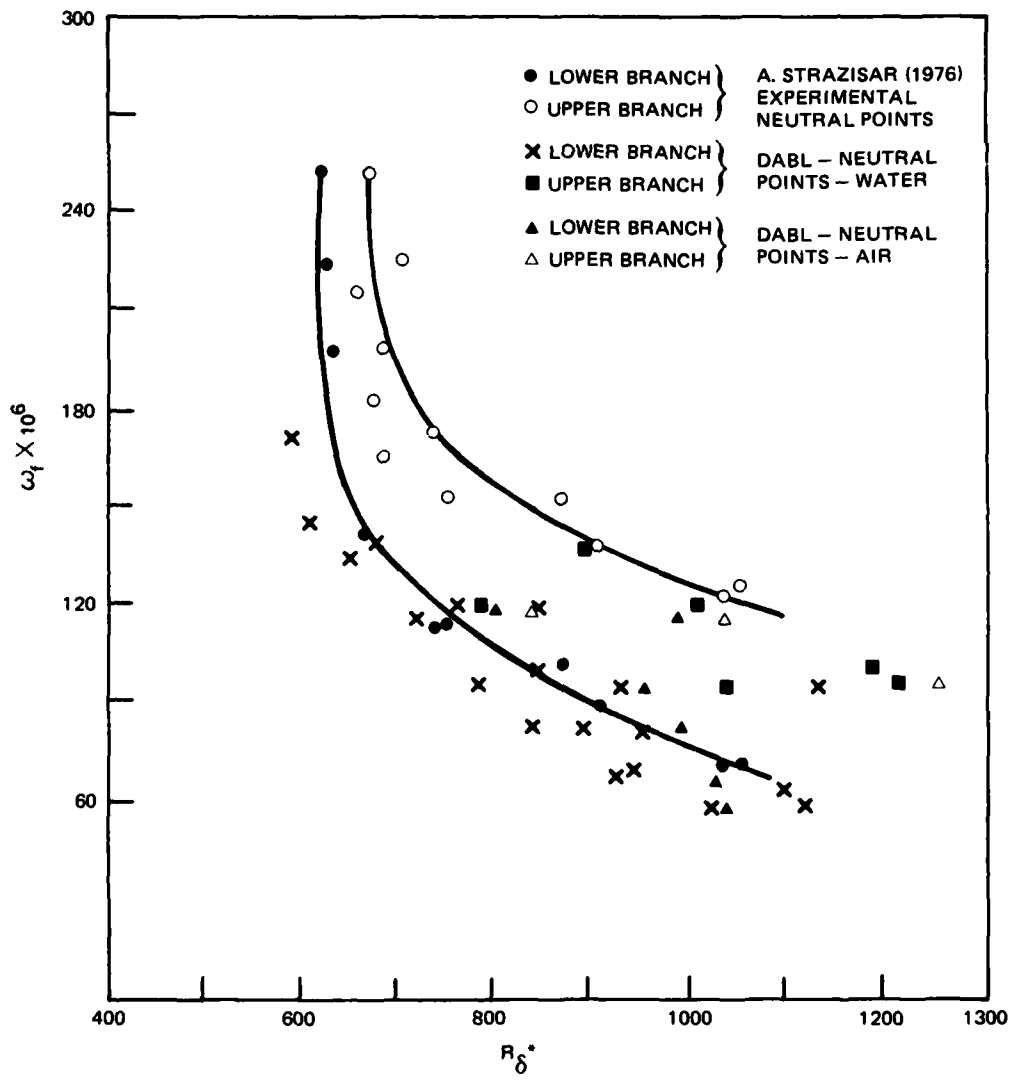


Figure 3. Comparison of the neutral stability points of a flat plate with 2.78°C surface overheat.

AXISYMMETRIC GEOMETRY

A 9:1 ellipsoid was selected to provide a comparison between the results of DABL and TAPS for both a heated and unheated axisymmetric body. The coordinates, potential flow velocities and surface temperature distribution of the ellipsoid are given in Appendix B while a comparison of the potential flow velocities computed by DABL and TAPS is shown in Figure 4.

First, for the unheated case, Figures 5, 6 and 7 compare the skin friction coefficient, boundary layer shape factor and displacement thickness Reynolds number as a function of arc length computed by DABL and TAPS at $R_L \cong 4.5 \times 10^6/\text{ft}$. In all cases there is good agreement between DABL and TAPS with slight differences occurring near the ellipsoid nose. Figures 8 and 9 compare the computed values of the disturbance growth rates for nondimensional frequencies $\omega_f = 0.32 \times 10^{-4}$ and $\omega_f = 0.486 \times 10^{-4}$, respectively. The corresponding amplification ratios are shown in Figure 10. Both the growth rates and amplification ratios of DABL and TAPS are in close agreement. It should be noted that the higher amplification ratios calculated by DABL are consistent with the results given by vonKerczek and Groves (1978).

For the heated case, the surface temperature distribution shown in Figure 11 was used by both DABL and TAPS for the ellipsoid at $R_L \cong 4.49 \times 10^6/\text{ft}$. Figures 12, 13 and 14 compare the skin friction coefficient, shape factor and displacement thickness Reynolds number computed by DABL and TAPS. The computed disturbance growth rates and amplification ratios for frequencies $\omega_f = 0.32 \times 10^{-4}$ and $\omega_f = 0.18 \times 10^{-4}$ are shown in Figures 15, 16 and 17. In all cases DABL produces larger growth rates and amplification ratios than TAPS. As stated by vonKerczek and Groves, linear stability theory is sensitive to the boundary layer shape factor and Figure 13 shows that DABL yields a slightly larger shape factor than TAPS which could account for the larger growth rates and amplification ratios. Figure 17 also compares the amplification ratios at $\omega_f = 0.22 \times 10^{-4}$ between DABL and TAPS and DABL's amplification ratios for a constant surface temperature difference, $\Delta T = 6.0\text{C}$. It can be concluded that DABL produces more conservative results as compared to TAPS.

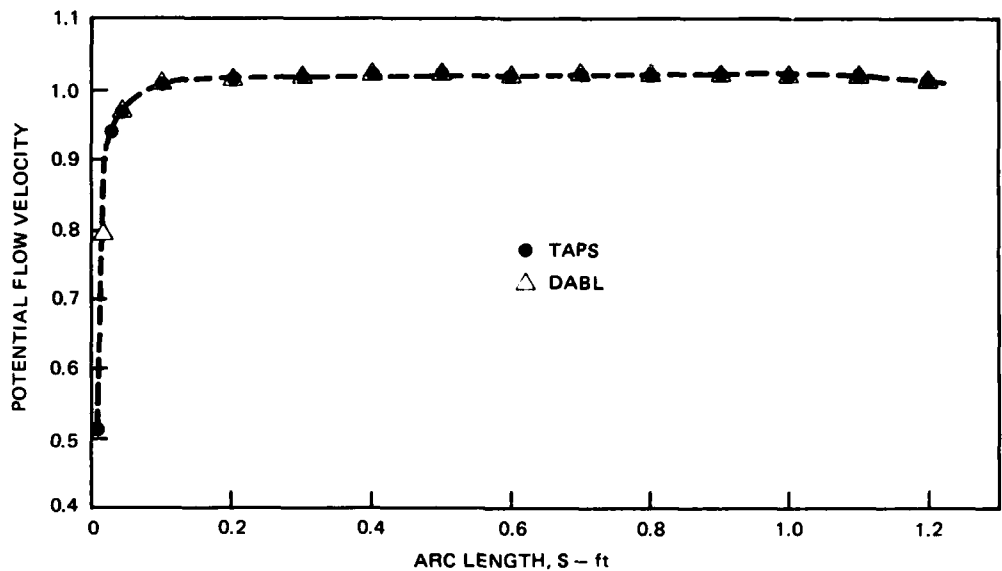


Figure 4. Potential flow velocity distribution of a 9:1 ellipsoid.

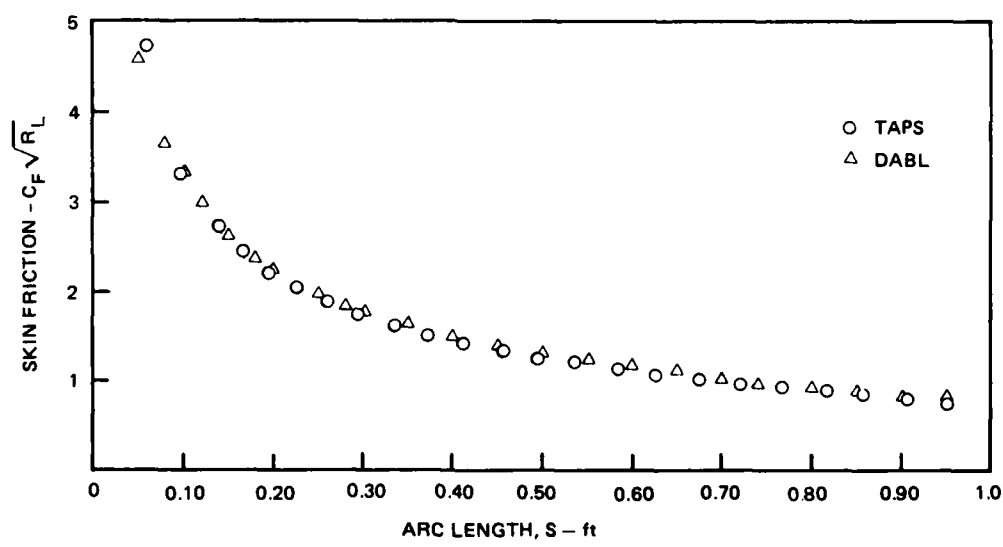


Figure 5. Skin friction coefficient of a 9:1 ellipsoid – $R_L = 4.5345455 \times 10^6/\text{ft}$.

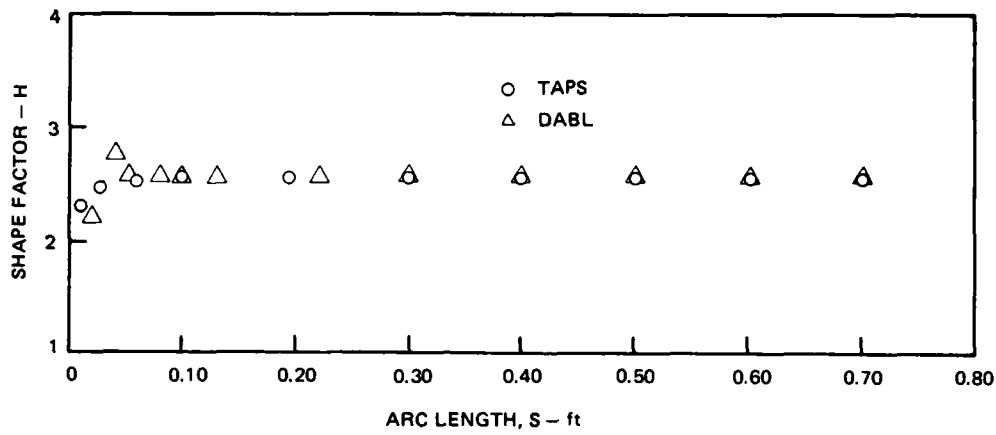


Figure 6. Boundary layer shape factor of a 9:1 ellipsoid – $R_L = 4.5345455 \times 10^6/\text{ft}$

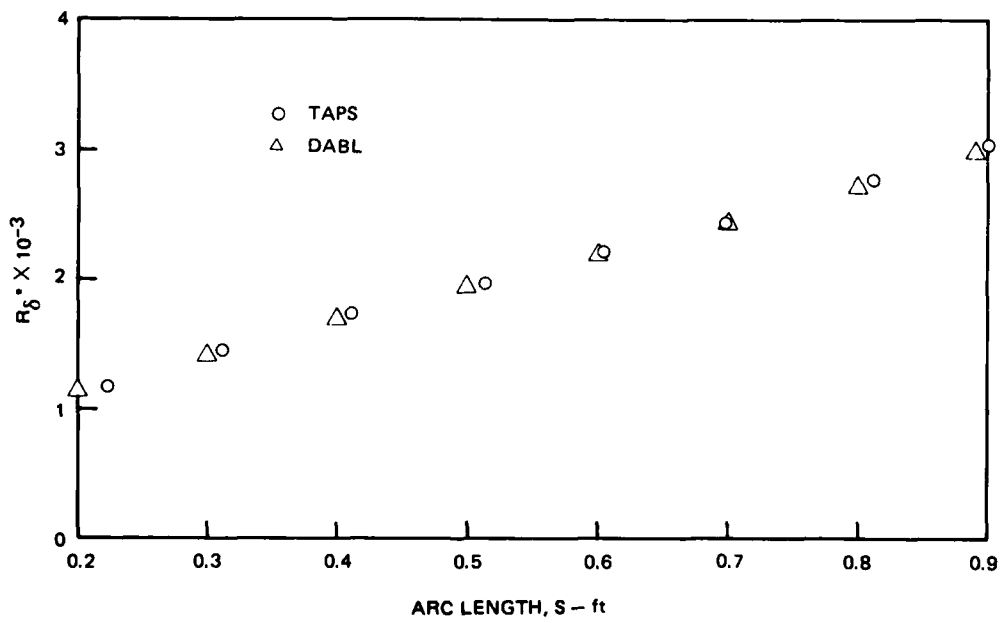


Figure 7. Displacement thickness Reynolds number of a 9:1 ellipsoid – $R_L = 4.5345455 \times 10^6/\text{ft}$.

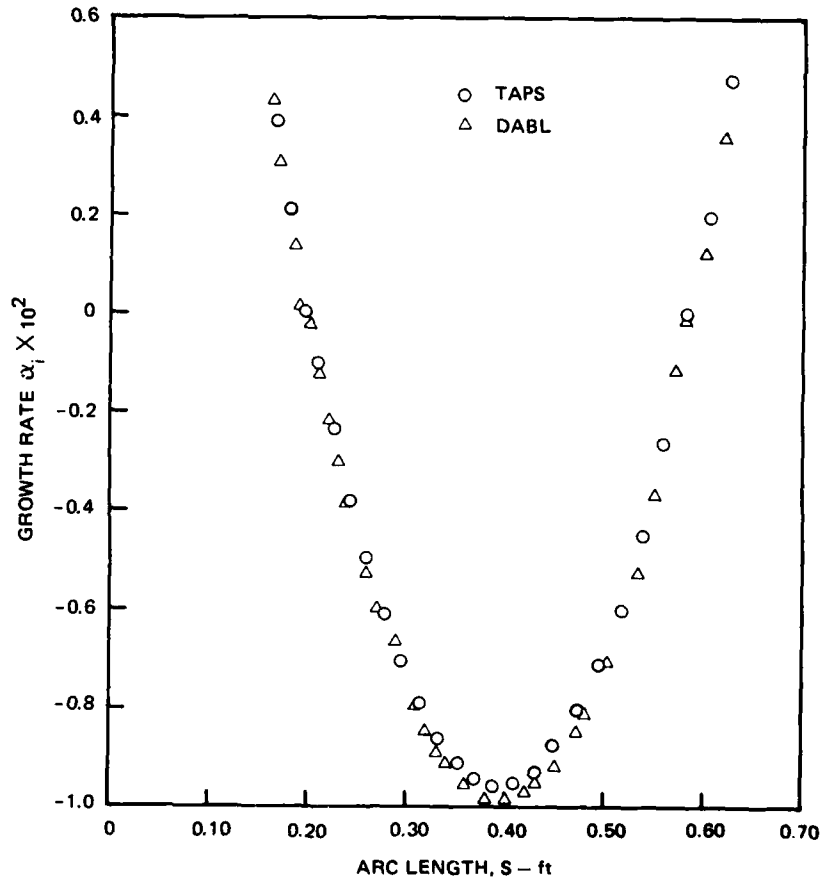


Figure 8. Computed growth rates of a 9:1 ellipsoid for
 $\omega_f = 0.486 \times 10^{-4}$ — $R_L = 4.5345455 \times 10^6/\text{ft}$.

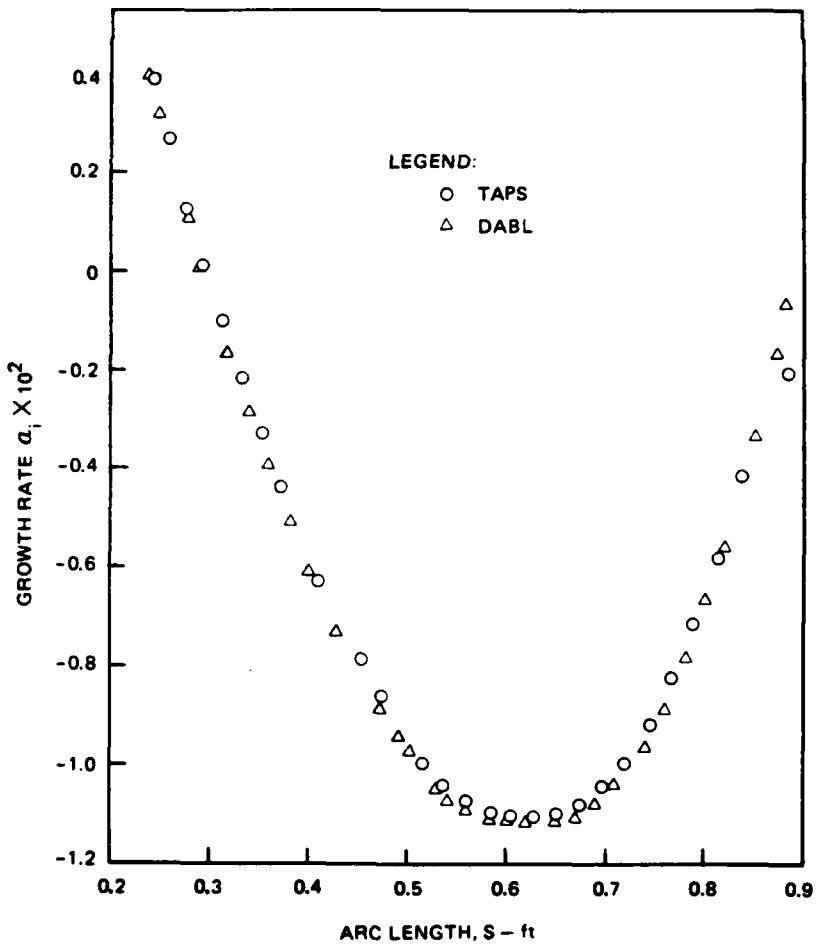


Figure 9. Computed growth rates of a 9:1 ellipsoid for
 $\omega_f = 0.32 \times 10^{-4}$ - $R_L = 4.5345455 \times 10^6/\text{ft}$.

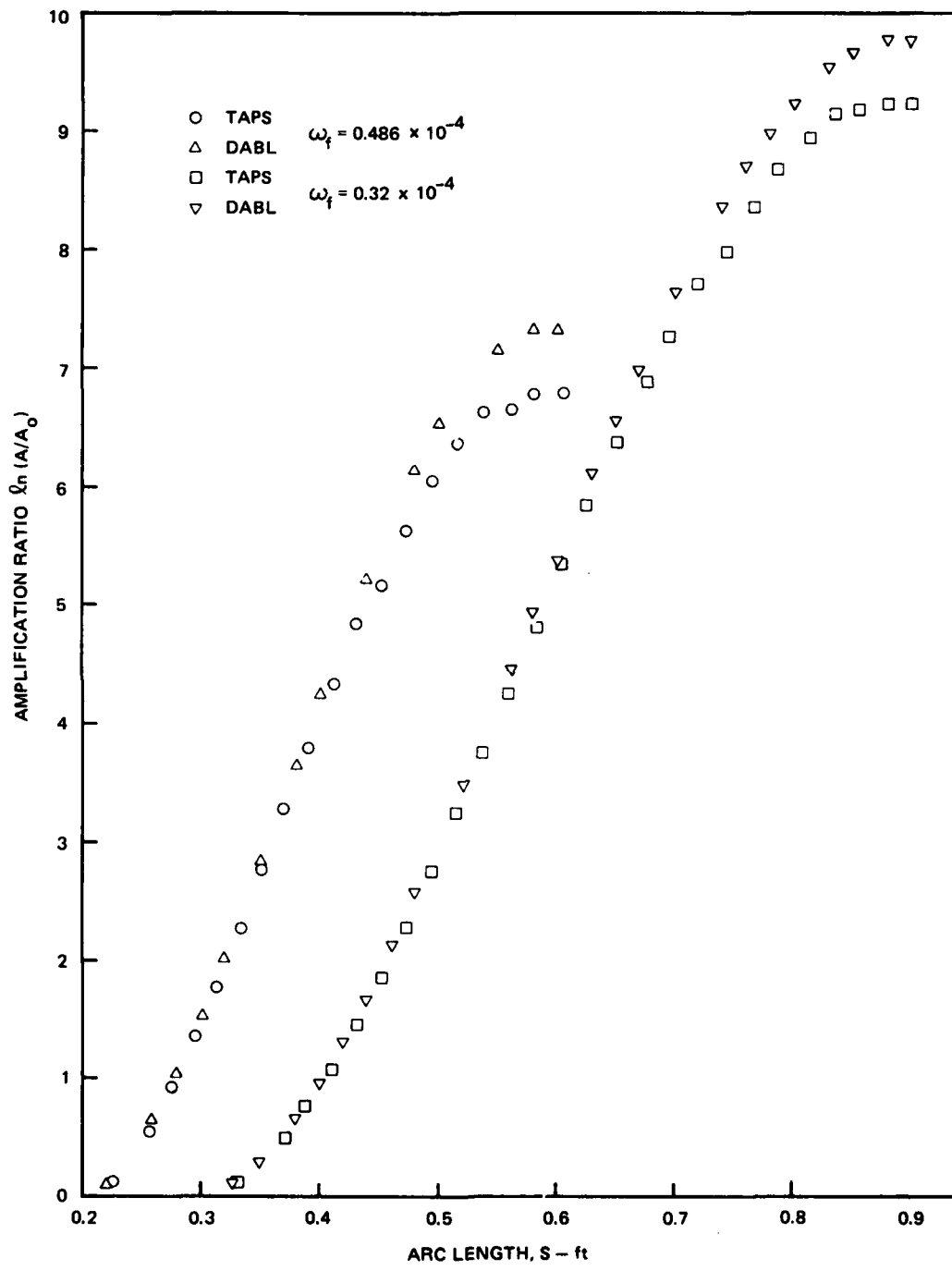


Figure 10. Comparison of the computed amplification ratios of a 9:1 ellipsoid for $\omega_f = 0.486 \times 10^{-4}$ and $\omega_f = 0.32 \times 10^{-4}$ — $R_L = 4.5345455 \times 10^6/\text{ft}$.

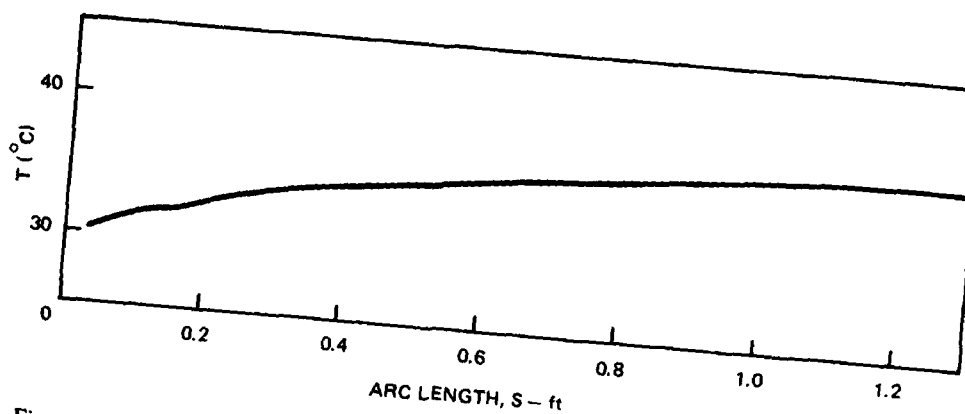


Figure 11. Surface temperature distribution of a 9:1 ellipsoid — $R_L = 4.4901734 \times 10^6/\text{ft}$.

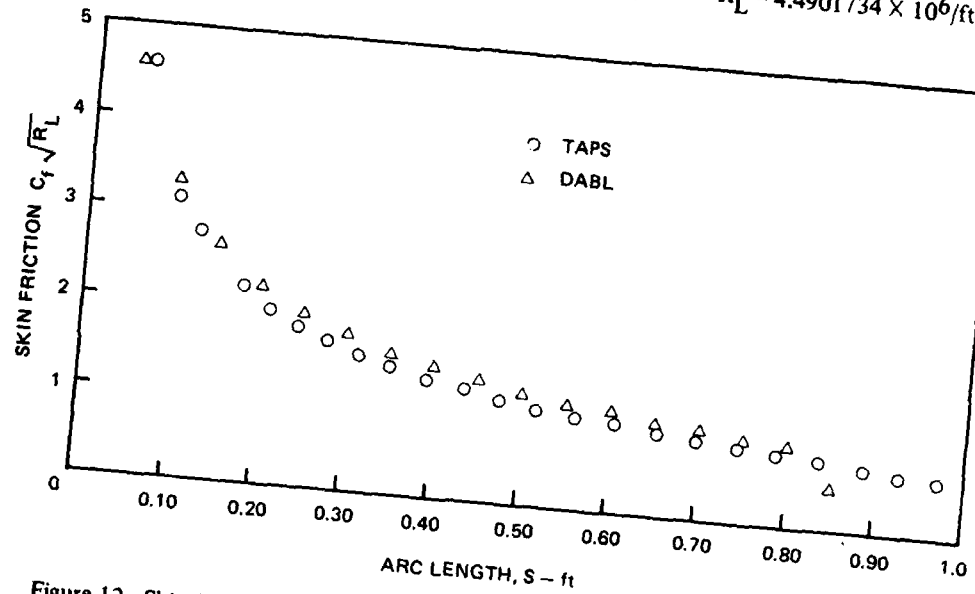


Figure 12. Skin friction coefficient of a heated 9:1 ellipsoid — $R_L = 4.4901734 \times 10^6/\text{ft}$.

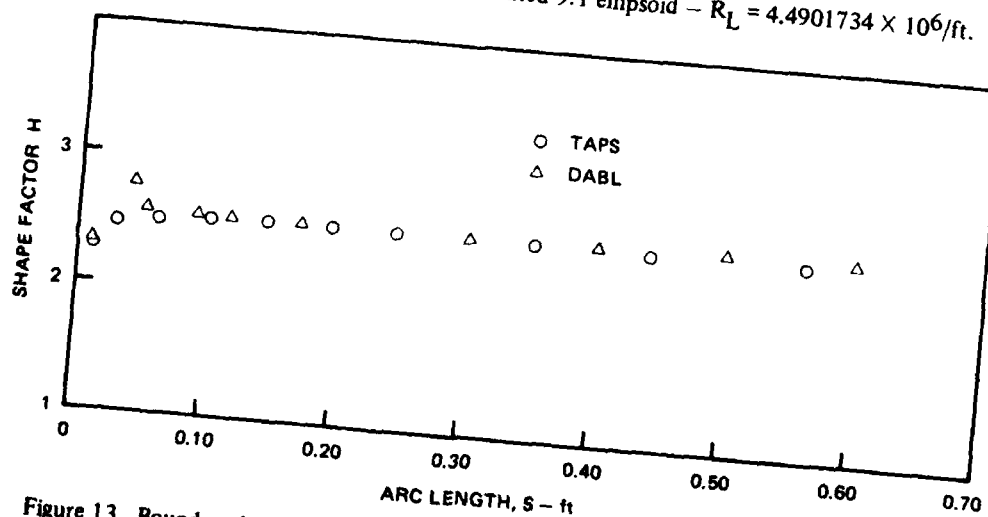


Figure 13. Boundary layer shape factor of a heated 9:1 ellipsoid — $R_L = 4.4901734 \times 10^6/\text{ft}$.

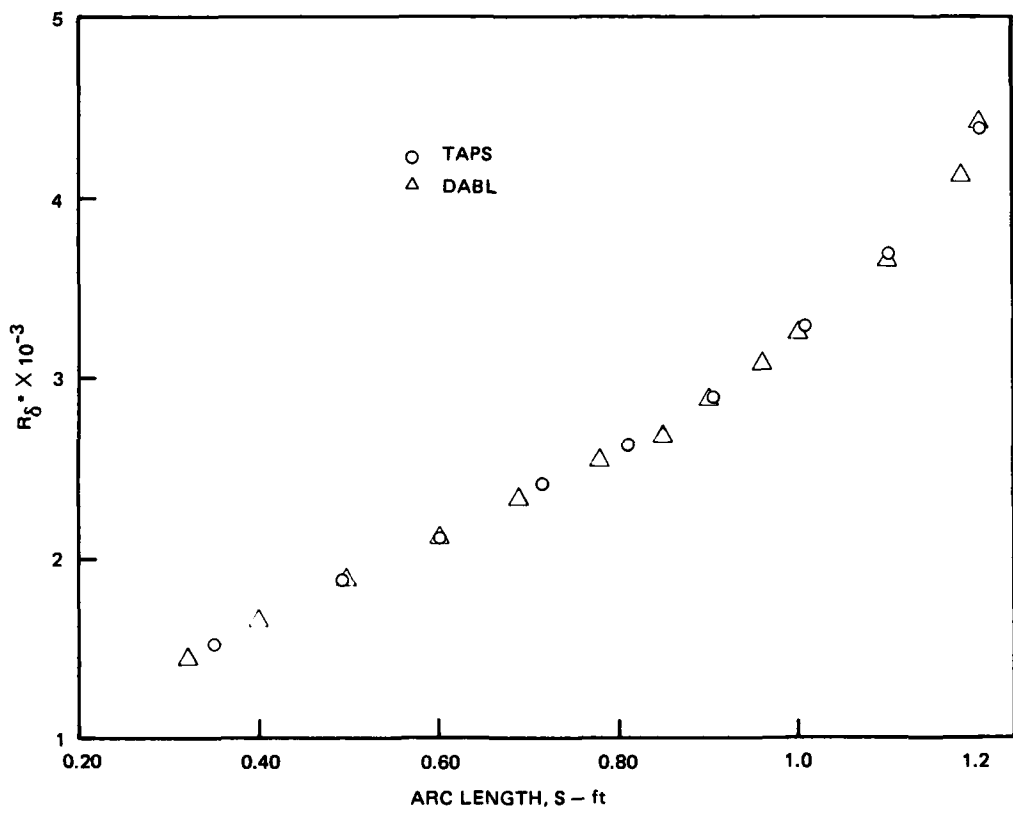


Figure 14. Displacement thickness Reynolds number of a heated 9:1 ellipsoid –
 $R_L = 4.4901734 \times 10^6/\text{ft.}$

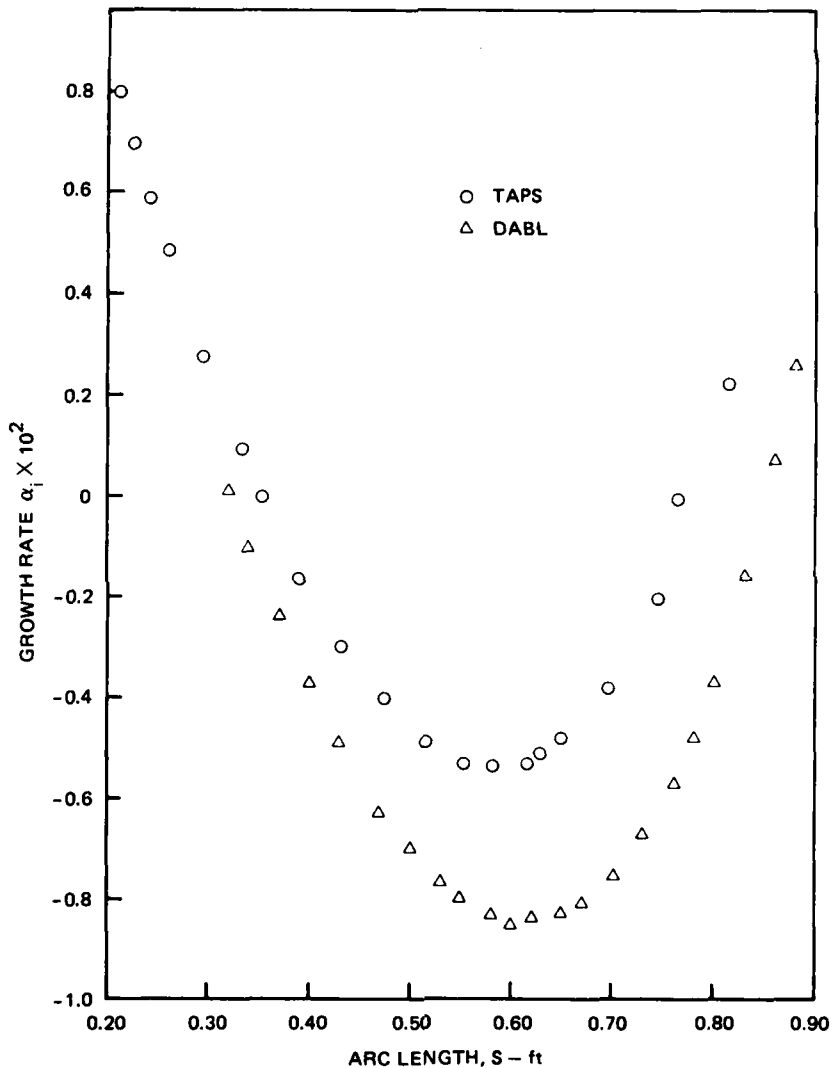


Figure 15. Computed growth rates of a heated 9:1 ellipsoid for
 $\omega_f = 0.32 \times 10^{-4}$ — $R_L = 4.4901134 \times 10^6/\text{ft}$.

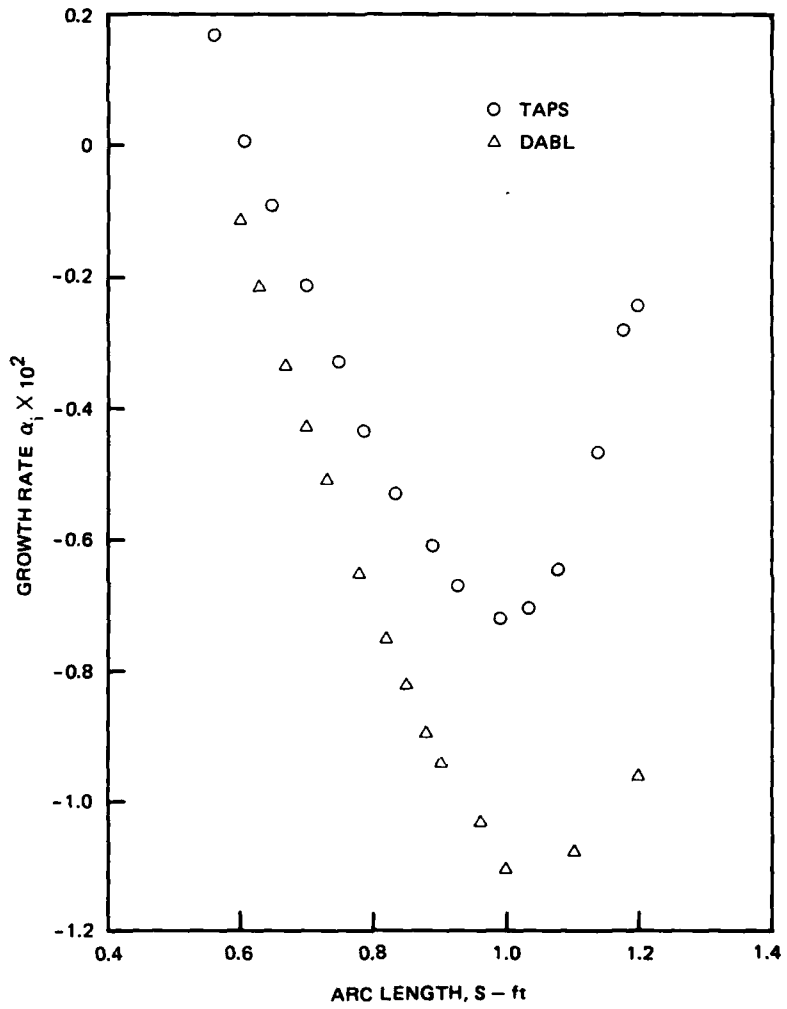


Figure 16. Computed growth rates of a heated 9:1 ellipsoid for
 $\omega_f = 0.18 \times 10^{-4}$ — $R_L = 4.4901734 \times 10^6/\text{ft}$.

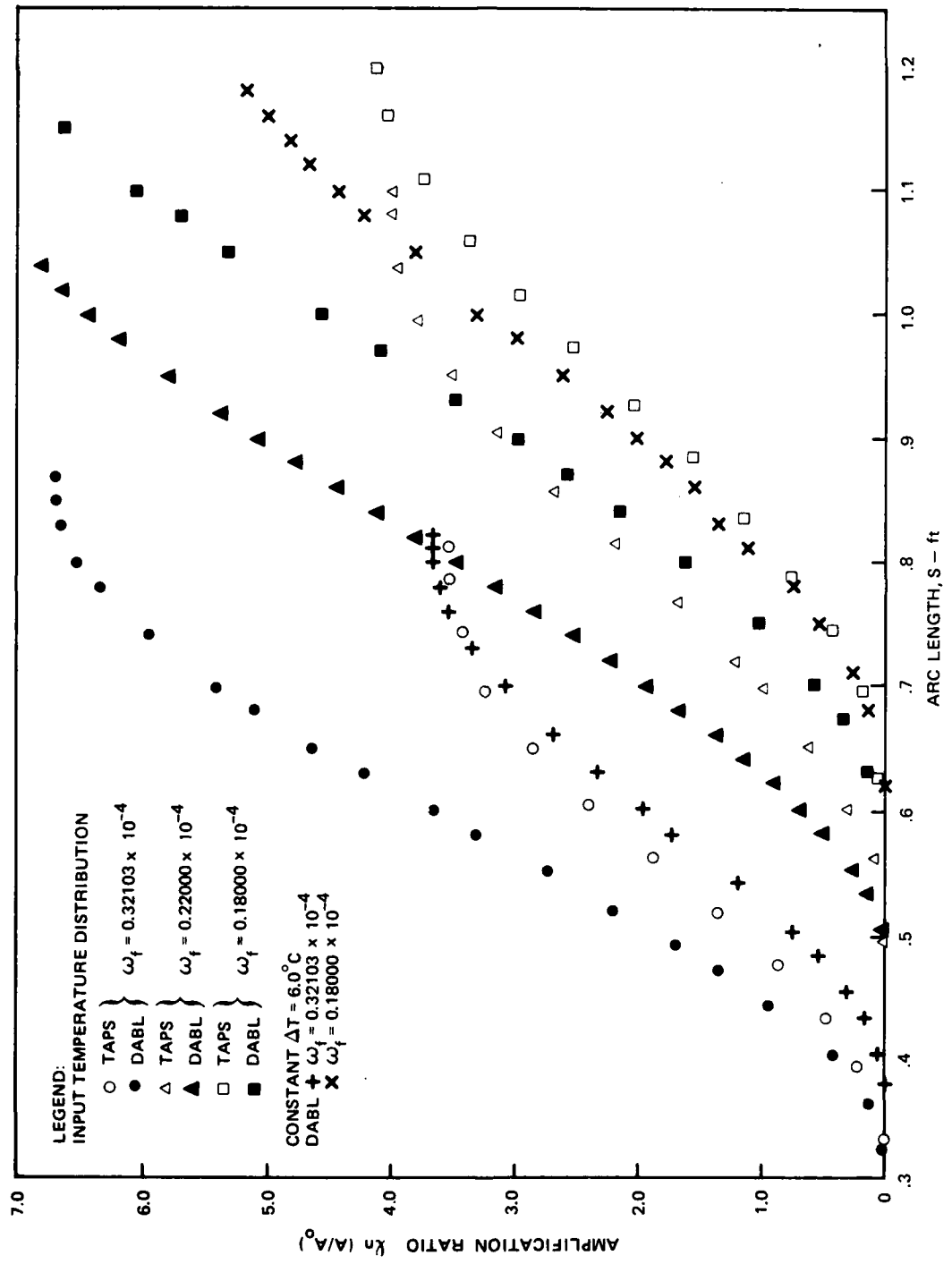


Figure 17. Comparison of the computed amplification ratios for a heated 9:1 ellipsoid – R_L = 4.4901734 × 10⁶/ft.

COMPUTER PROGRAM USAGE

DEFINITION OF THE INPUT VARIABLES

VARIABLE	DESCRIPTION
IBL	If IBL = 0, calculate the boundary layer properties and perform the stability analysis If IBL = 1, calculate the boundary layer properties to separation or the end of the body
IBLTP	If IBLTP = 0, do not read or write boundary layer data to unit 8 If IBLTP = 1, write boundary layer data to unit 8 If IBLTP = 2, read boundary layer data from Unit 8
IHEAT	If IHEAT = 0, unheated boundary layer If IHEAT = 1, heated boundary layer
IPOT	If IPOT = 0, calculate potential flow If IPOT = 1, calculate potential flow and punch cards If IPOT = 2, input potential flow according to Data Table 4
ISTART	If ISTART = 0, automatic start of the stability analysis If ISTART = 1, the user provides information – Data Table 2 – for starting/restarting the stability calculations
ITWOD	If ITWOD = 0, axisymmetric body If ITWOD = 1, 2-D body's lower surface If ITWOD = 2, 2-D body's upper surface
IFIT	IFIT controls the amount of boundary layer velocity and temperature profile data used in the stability analysis at each station If IFIT = 1, use every point – normal option If IFIT = 2, use every second point, etc.
IKFZ	If IKFZ = 0, stability analysis stops when the disturbances no longer experience amplification If IKFZ = 1, stability analysis proceeds regardless of amplification
IVISC	If IVISC = 1, water boundary layer If IVISC = 2, air boundary layer
NP	Number of body offsets NP ≤ 160 axisymmetric body NP ≤ 101 2-D body
IBEG	If IBEG = 0, stability analysis autostart begins at station 1 If IBEG ≠ 0, stability analysis autostart begins at station X(IBEG)

VARIABLE	DESCRIPTION
KF	The number of nondimensional frequencies for which the amplification ratio is computed If ISTART = 0, $3 \leq KF \leq 10$ If ISTART = 1, $1 \leq KF \leq 10$ $\omega_f)_{i+1} = 0.83 \omega_f)_i$
BEPS	The convergence criteria in the iteration for the stagnation point in the boundary layer code BEPS = 0.0001 is the recommended value
BLDELS	Arc length increment to be used in the boundary layer calculation
DELS	The estimated arc length spacing at which the instability growth rates are to be computed. The program varies DELS as needed.
TOL	The accuracy to be maintained in the integration of the stability equation TOL = 0.001 is the recommended value
EPS	The convergence criteria for the eigenvalue integration EPS = 0.001 is the recommended value
X	Input abscissa
Y	Input ordinate
OMU	Nondimensional frequency ω_f for which the amplification ratios are to be computed
SO	Arc length starting values for the stability calculations corresponding to OMU
RL	Reynolds number = $U_\infty L / \nu_\infty$ Where U_∞ is the free stream velocity (ft/sec); ν_∞ is the kinematic viscosity (ft ² /sec); L is a reference length
ANORM	A normalization factor; the X, Y input offsets are divided by ANORM
R1	Displacement thickness Reynolds number at the last completed station; it is input only when restarting the stability calculations – ISTART = 1 If ISTART = 0; R1 = 0
U1	Potential flow surface velocity at the last completed station; it is input only when restarting the stability calculations – ISTART = 1 If ISTART = 0, U1 = 0
JMAX	The number of points across the boundary layer at which the velocity profiles are computed JMAX ≤ 201 JMAX = 201 is the recommended value
ETA	The scaled edge of the boundary layer ETA = 6.0 is the normal input
ALFRU	The starting estimate or the value at the last completed station SO for the wave number (α_r^*); it cannot be zero and is usually less than 0.5 for a starting estimate

VARIABLE	DESCRIPTION
ALFIU	The starting estimate or the value at the last completed station SO for the disturbance growth rate (α_i^*); a value of zero will usually suffice as a starting estimate
AMP	The value of the amplification ratio at the last completed station SO or zero for a starting estimate
ITT	A control for the type of temperature distribution If ITT = 0, no heating If ITT = 1, a step function temperature distribution If ITT = 2, a linear temperature distribution If ITT = 3, temperature is given at each input x offset
ITEMP1	The station number corresponding to the offset at which the surface temperature variation is to begin If ITT = 3, ITEMPI = 0
ITEMP2	The station number corresponding to the offset at which the surface temperature variation is to end If ITT = 3, ITEMPI = 0
TEMPI	The free stream temperature in degrees Celsius
DTEMP	The difference in temperature ΔT in Celsius between the free stream temperature and the maximum body temperature If ITT = 3, DTEMP = 0
T	The body temperature corresponding to the x input offsets
UB	The potential flow surface velocities
XC	The scaled abscissa corresponding to the maximum 2-D body diameter
YC	The scaled ordinate corresponding to the midpoint of the maximum diameter
ANGO	The angle of attack in radians

METHOD OF INPUTTING DATA TABLES

The input data tables of body coordinates, temperature distribution and potential flow are input as shown below.

Body Coordinates

Card Columns	F Format					
	1 - 10	11 - 20	21 - 30	31 - 40	41 - 50	51 - 60
X ₁	X ₂	X ₃
...	X _{NP}			
Y ₁	Y ₂	Y ₃
...	Y _{NP}			

Temperature Distribution

Card Columns	F Format					
	1 - 10	11 - 20	21 - 30	31 - 40	41 - 50	51 - 60
	T ₁	T ₂	T ₃
	T _{NP}		

Potential Flow Surface Velocities

Card Columns	F Format					
	1 - 10	11 - 20	21 - 30	31 - 40	41 - 50	51 - 60
	UB ₁	UB ₂	UB ₃
	UB _{NP-1}		

PROGRAM INPUT SCHEME

Label Card

Card Columns	Format	Variable
1 - 60	A	TITLE

Flag Card

Card Columns	Format	Variable
1	I	IBL
3	I	IBLTP
5	I	IHEAT
7	I	IPOT
9	I	ISTART
11	I	ITWOD
13	I	IFIT
15	I	IKFZ
17	I	IVISC
19 - 21	I	NP
23 - 25	I	IBEG
27 - 29	I	KF

Constant Card 1

Card Columns	Format	Variable
1 - 20	F	RL
21 - 30	F	ANORM
31 - 40	F	R1
41 - 50	F	U1

Constant Card 2

Card Columns	Format	Variable
1 - 3	I	JMAX
11 - 20	F	ETA
21 - 30	F	BEPS
31 - 40	F	BLDELS
41 - 50	F	DELS
51 - 60	F	TOL
61 - 70	F	EPS

Data Table 1: Body Coordinates $Y = f(x)$

The maximum number of entries this table may contain is:

- NP = 160 for an axisymmetric body
- NP = 101 for a two-dimensional body

Figure 18 illustrates the method used to input the coordinates for an axisymmetric body while Figure 19 should be used for two-dimensional bodies.

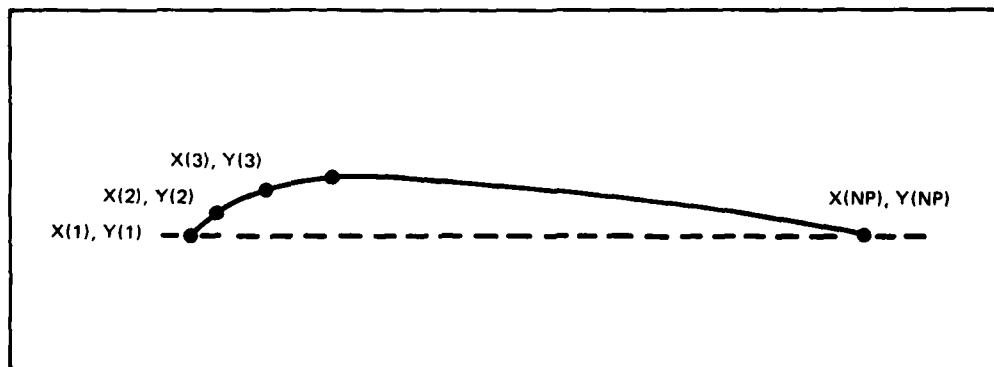


Figure 18. Input direction for the axisymmetric body coordinates.

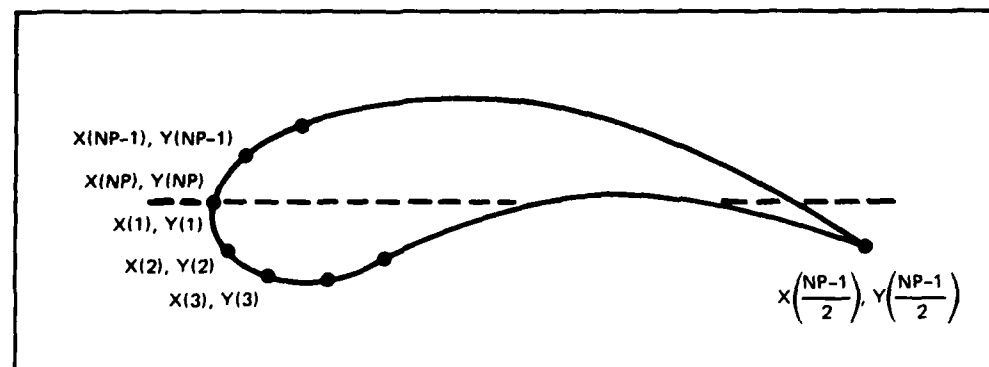


Figure 19. Input direction for the two-dimensional body coordinates.

Data Table 2: Start/Restart Information for the Stability Calculations

If ISTART = 0, do not input this table. The number of entries is $1 \leq KF \leq 10$.

Card Columns	Format	Variable
1 - 10	E	OMU(I)*
11 - 20	F	SO(I)
21 - 30	F	ALFRU(I)
31 - 40	F	ALFIU(I)
41 - 50	F	AMP(I)

*Note: Repeat this card for each value of OMU ($I = 1, KF$).

Constant Card 3

If IHEAT = 0, do not input this card.

Card Columns	Format	Variable
1	I	ITT
3 - 5	I	ITEMP1
7 - 9	I	ITEMP2
11 - 20	F	TEMP1
21 - 30	F	DTEMP

Data Table 3: Body Surface Temperature Distribution $T = f(x)$

If IHEAT = 0 or ITT $\neq 3$, do not input this table.

The number of entries in this table is NP.

Each input temperature corresponds to each input x offset - Data Table 1.

For two-dimensional bodies, the surface temperature distribution follows the input scheme of Figure 19.

Data Table 4: Potential Flow Surface Velocities $UB = f(x)$

The number of entries in this table is $NP-1$.

The potential flow velocities are at the midpoints of the input x offsets — Data Table 1.

For two-dimensional bodies, the potential flow velocities follow the input scheme of Figure 19.

Constant Card 4

If $IPOT = 2$ and $ITWOD = 0$, do not input this card.

Card Columns	Format	Variable
1 - 10	F	XC
11 - 20	F	YC
21 - 30	F	ANGO

COMPUTER PRINTOUT**INCLUDED ITEMS**

All input quantities are printed out to allow for rapid checking for errors. The following section contains the definitions of those output variables not previously defined. Below is a list of the items included in the program output.

1. Control parameters
2. Input body coordinates
3. Start/Restart variables for the stability calculations ($ISTART = 1$)
4. Temperature control variables
5. Input temperature distribution ($IHEAT = 1$, $ITT = 3$)
6. Normalized body coordinates and temperature distribution ($IHEAT = 1$)
7. Boundary layer parameters
8. Stability autostart variables ($ISTART = 0$)
9. Stability calculations ($IBL = 0$)

PRINTOUT DEFINITIONS**Boundary Layer Parameters**

VARIABLE	DEFINITION
S	The computed arc length values at which the boundary layer calculations are made
UEF	Potential flow surface velocity
DUE	Derivatives of the potential flow surface velocity with respect to arc length
RADIUS	Body radius

VARIABLE	DEFINITION
BETA	The Hartree parameter
GAMMA	A boundary layer scale factor
DELTN	Nondimensional boundary layer thickness times $\sqrt{R_L}$
DI	Nondimensional displacement thickness times $\sqrt{R_L}$
H	The boundary layer shape factor
CT	The wall skin friction coefficient times $\sqrt{R_L}$
CQ	Nondimensional local heat transfer coefficient divided by $\sqrt{R_L}$
VISCR	The ratio of fluid viscosity at the wall to that of the ambient fluid

Note: To obtain the actual value of the nondimensional boundary layer thickness, displacement thickness, skin friction coefficient and heat transfer coefficient, divide DELTN, DI and CT by $\sqrt{R_L}$ and multiply CQ by $\sqrt{R_L}$.

Stability Automatic Start

VARIABLE	DEFINITION
S	The arc length
RC	The critical displacement thickness Reynolds number
RD	The displacement thickness Reynolds number
ALPHAC	The critical value α_c of α
OMEGAC	The critical frequency associated with the critical displacement thickness Reynolds number

Stability Calculations

VARIABLE	DEFINITIONS
S	The arc length
U	The potential flow surface velocity
H	The boundary shape factor
DI	The nondimensional displacement thickness times $\sqrt{R_L}$
CT	The wall skin friction coefficient times $\sqrt{R_L}$
R	The displacement thickness Reynolds number
XI	A boundary layer scale factor
RADIUS	The body radius
OMU	The nondimensional frequency $- \omega_f$
ALFRU	The real part of the complex wave number $- \alpha^*$

VARIABLE	DEFINITIONS
ALFIU	The relative growth rate of the disturbance – imaginary part of α^*
AMP	The amplification ratio A/A_0
ITER	The number of times the eigenvalue problem is solved
NSTEP	The number of integration steps of the Orr-Sommerfeld integration

Note: The DABL code solves the adjoint Orr-Sommerfeld problem where the complex conjugate of α is the eigenvalue. Therefore the output yields

$$\text{ALFRIU} \equiv \text{Im}(\alpha^*) \begin{cases} < 0 & \text{Damped} \\ = 0 & \text{Neutral} \\ > 0 & \text{Amplified} \end{cases} \quad \left. \right\} \text{Disturbance}$$

SUMMARY

Several examples illustrating the use of DABL for heated and unheated, two-dimensional and axisymmetric bodies have been presented. For both a heated and unheated flat plate, DABL's automatic starting mode calculated nondimensional frequencies which resulted in neutral stability points falling within the previously defined neutral curves. In general, DABL produces unconservative neutral point estimates for the unheated plate and conservative estimates for the heated plate. However, for the unheated plate, when the Reynolds number and disturbance frequencies are reduced, the results fall closer to the neutral curve. Also, the amplification ratios calculated by DABL, for the unheated plate, compare favorably with published results.

The boundary layer properties, growth rates and amplification ratios computed by DABL for an unheated 9:1 ellipsoid compare favorably with the results of TAPS. However, for the heated 9:1 ellipsoid, DABL consistently calculated larger growth rates and amplification ratios than TAPS even though there is close agreement in the calculated boundary layer properties. From these results it can be concluded that DABL produces conservative results for heated axisymmetric bodies.

The DABL computer code can be considered an effective tool in performing parametric design studies for both heated and unheated bodies. For unheated bodies, DABL can be used for predicting the location of boundary layer transition by the e^N method. With its straight forward input scheme, DABL is easy to use and requires a minimum of user interaction.

REFERENCES

1. C. Basset, Private communication – TAPS computations.
2. J. P. Giesing, Extension of the Douglas Neuman Program to Problems of Lifting, Infinite Cascades, Douglas Aircraft Report LB31653 (1964).
3. R. Jordinson, The Flat Plate Boundary Layer. Part 1. Numerical Integration of the Orr-Sommerfeld Equation, Journal of Fluid Mechanics, Vol. 43, Part 4, pp. 801–811 (1970).
4. J. A. Ross, R. H. Barnes, J. G. Burns and M. A. S. Ross, The Flat Plate Boundary Layer. Part 3. Comparison of Theory with Experiment, Journal of Fluid Mechanics, Vol. 43, Part 4, pp. 819–832 (1970).
5. G. B. Schubauer and H. K. Skramstad, Laminar Boundary Layer Oscillations and Transition on a Flat Plate, NACA Report 909 (1948).
6. A. J. Strazisar, Experimental Study of the Stability of Heated Laminar Boundary Layers in Water, PhD thesis, Case Western Reserve University (1976).
7. C. vonKerczek and N. C. Groves, Disturbance Amplification in Boundary Layers, DTNSRDC Report 78/004 (1978).

APPENDIX A

This appendix contains an abbreviated computer printout of the automatic start — stability analysis of a heated flat plate.

DABL - 9:1 ELLIPSOID - HEATED

CONTROL PARAMETERS

I3L = 0 IBLTP = 0 IHEAT = 1 IPOTS = 2
ISTART = 1 ITWOD = 0 IFIT = 1 IKFZ = 0 IVISC = 1
IIP = 04 IREG = 0 KF = 2

PI = 4490173.3750 ANORM = 1.000000

UMAX = 201 ETAS = 5.000000 DEPS = .001000 ALDELS = .005000
DELSE = .001000 TOL = .701000 EPS = .001000

INPUT BODY COORDINATES

X Y

.00000	.00000
.29813-001	.19147-001
.41647-001	.27167-001
.62500-001	.33029-001
.93333-001	.37057-001
.10417+000	.42008-001
.12500+000	.45667-001
.14583+000	.48644-001
.16647+000	.51912-001
.18750+000	.54621-001
.20833+000	.57102-001
.22917+000	.59402-001
.25000+000	.61523-001
.27083+000	.63489-001
.29167+000	.65314-001
.31250+000	.67007-001
.33333+000	.68585-001
.35417+000	.70044-001
.37500+000	.71407-001
.39583+000	.72466-001
.41667+000	.73832-001
.43750+000	.74908-001
.45833+000	.75898-001
.47917+000	.76806-001
.50000+000	.77434-001
.52083+000	.78184-001
.54167+000	.79061-001
.	.
.	.
.	.

THIS PAGE IS BEST QUALITY PRACTICABLE
FROM COPY

RESTART OF THE STABILITY CALCULATIONS

R1= 1880.000 U1= 1.020

I= 1	04U111=	.321n00-004	50=	.50000	ALFRU111=	.19211	ALFIU=	.00700	AMP111=	1.87100
I= 2	04U111=	.220n00-004	50=	.50000	ALFRU111=	.20000	ALFIU=	.00000	AMP111=	.00000

BODY BOUNDARY LAYER = HEATED

ITT= 3 TEMP1= 10.10000 DTEMP= 7.37000 ITMP1= 1 ITMP2= 84

INPUT TEMPERATURE DISTRIBUTION

X	TEMP
.00000	.30n40+002
.20813+001	.30n40+002
.41647+001	.30n00+002
.62500+001	.31n00+002
.81333+001	.31n00+002
.10017+000	.31740+002
.12500+000	.31n60+002
.14583+000	.32nn0+002
.16667+000	.32400+002
.18750+000	.32700+002
.20813+000	.33160+002
.22917+000	.33250+002
.25000+000	.33600+002
.27083+000	.33700+002
.29117+000	.33850+002
.31250+000	.34070+002
.33333+000	.34250+002
.35417+000	.34330+002
.37500+000	.34450+002
.39583+000	.34400+002
.41667+000	.34700+002
.43750+000	.34830+002
.45813+000	.34700+002
.47917+000	.35n50+002
•	•
•	•

POTENTIAL FLOW SOLUTION AND TEMPERATURE DISTRIBUTION
 $X = X/\Delta H_{\text{norm}}$, $Y = Y/\Delta H_{\text{norm}}$

X	Y	S	U	T
.00000	.00000	.+14216-001	.79461+000	.30040+002
.20833-001	.19349-001	.+39559-001	.97418+000	.30040+002
.41667-001	.27167-001	.+61506-001	.98902+000	.30270+002
.62500-001	.33027-001	.+83019-001	.99927+000	.30750+002
.83333-001	.37857-001	.+10433+000	.+10055+001	.31200+002
.10417+000	.42000-001	.+12553+000	.+10096+001	.31570+002
.12500+000	.45667-001	.+14665+000	.+10124+001	.31800+002
.14583+000	.48944-001	.+16772+000	.+10145+001	.31930+002
.16667+000	.51912-001	.+18875+000	.+10161+001	.32200+002
.18750+000	.54621-001	.+20974+000	.+10173+001	.32550+002
.20833+000	.57109-001	.+23071+000	.+10184+001	.32930+002
.22917+000	.59402-001	.+25166+000	.+10192+001	.33205+002
.25000+000	.61523-001	.+27259+000	.+10199+001	.33375+002
.27083+000	.63489-001	.+29351+000	.+10206+001	.33600+002
.29167+000	.65314-001	.+31442+000	.+10211+001	.33775+002
.31250+000	.67009-001	.+33532+000	.+10215+001	.33960+002
.33333+000	.68585-001	.+35621+000	.+10219+001	.34160+002
.35417+000	.70048-001	.+37709+000	.+10222+001	.34290+002
.37500+000	.71407-001	.+39796+000	.+10225+001	.34390+002
.39583+000	.72668-001	.+41883+000	.+10228+001	.34525+002
.41667+000	.73837-001	.+43970+000	.+10230+001	.34650+002
.43750+000	.74908-001	.+46056+000	.+10232+001	.34745+002

THIS PAGE IS PROVIDED AS A REFERENCE
 FROM COPY FURNISHED TO BDC

.45833+000	.75898-001	.48141+000	.10234+001	.34865+002
.47917+000	.76806-001	.50226+000	.10235+001	.34975+002
.50000+000	.77634-001	.52311+000	.10237+001	.35100+002
.52083+000	.78385-001	.54395+000	.10238+001	.35200+002
.54167+000	.79061-001	.56480+000	.10239+001	.35300+002
.56250+000	.79664-001	.58564+000	.10239+001	.35400+002
.58333+000	.80196-001	.60648+000	.10240+001	.35475+002
.60417+000	.80658-001	.62732+000	.10241+001	.35575+002
.62500+000	.81051-001	.64815+000	.10241+001	.35700+002
.64583+000	.81376-001	.66899+000	.10241+001	.35785+002
.66667+000	.81635-001	.68982+000	.10241+001	.35860+002
.68750+000	.81827-001	.71066+000	.10241+001	.35925+002
.70833+000	.81954-001	.73149+000	.10241+001	.36000+002
.72917+000	.82015-001	.75232+000	.10241+001	.36085+002
.75000+000	.82010-001	.77316+000	.10241+001	.36160+002
.77083+000	.81941-001	.79399+000	.10240+001	.36235+002
.79167+000	.81805-001	.81482+000	.10239+001	.36310+002
.81250+000	.81604-001	.83566+000	.10239+001	.36385+002
.83333+000	.81337-001	.85649+000	.10238+001	.36450+002
.85417+000	.81002-001	.87733+000	.10236+001	.36490+002
.87500+000	.80600-001	.89817+000	.10235+001	.36550+002
.89583+000	.80129-001	.91701+000	.10234+001	.36650+002
.91667+000	.79587-001	.93785+000	.10232+001	.36725+002
.93750+000	.78775-001	.96049+000	.10230+001	.36775+002
.95833+000	.78289-001	.98154+000	.10227+001	.36850+002
.97917+000	.77527-001	.10024+001	.10224+001	.36930+002
.10000+001	.76689-001	.10232+001	.10221+001	.36980+002
.10208+001	.75770-001	.10441+001	.10218+001	.37065+002
.10417+001	.74767-001			.37165+002

.10625+001	.73681+001	.10650+001	.10213+001	.37225+002
.10833+001	.72503+001	.10858+001	.10208+001	.37300+002
.11042+001	.71231+001	.11067+001	.10202+001	.37410+002
.11250+001	.69059+001	.11276+001	.10176+001	.37470+002
.11458+001	.68381+001	.11484+001	.10188+001	.37470+002
.11667+001	.66790+001	.11693+001	.10178+001	.37470+002
.11875+001	.65077+001	.11902+001	.10167+001	.37470+002
.12083+001	.61234+001	.12111+001	.10153+001	.37470+002
.12292+001	.61249+001	.12321+001	.10137+001	.37470+002
.12500+001	.59106+001	.12530+001	.10119+001	.37470+002
.12708+001	.56788+001	.12740+001	.10105+001	.37470+002
.12917+001	.54222+001	.12949+001	.10170+001	.37470+002
.12957+001	.53375+001	.13076+001	.98470+000	.37470+002
.13126+001	.51017+001	.13182+001	.97726+000	.37470+002
.13292+001	.48458+001	.13350+001	.97141+000	.37470+002
.13457+001	.46300+001	.13516+001	.95796+000	.37470+002
.13626+001	.43942+001	.13687+001	.93382+000	.37470+002
.13793+001	.41667+001	.13855+001	.90911+000	.37470+002
.14167+001	.41667+001	.14126+001	.92730+000	.37470+002
.14683+001	.41667+001	.14522+001	.97101+000	.37470+002
.15000+001	.41667+001	.14938+001	.98399+000	.37470+002
.15417+001	.41667+001	.15355+001	.99044+000	.37470+002
.15833+001	.41667+001	.15772+001	.99478+000	.37470+002
.16250+001	.41667+001	.16189+001	.99797+000	.37470+002
.16667+001	.41667+001	.16605+001	.10002+001	.37470+002
.17083+001	.41667+001	.17022+001	.10035+001	.37470+002
.17500+001	.41667+001	.17438+001	.10067+001	.37470+002
.17917+001	.41667+001	.17855+001	.10110+001	.37470+002
		.18272+001	.10176+001	.37470+002

THIS PAGE IS BASED QUALITY PRACTICABLE
FROM COPY FROM THE PC

CONSTANT BOUNDARY LAYER/STABILITY ANALYSIS

• 41667-001	• 19888+001	• 102008+001	• 37470+002
• 41667-001	• 19105+001	• 10489+001	• 37470+002
• 41667-001	• 19522+001	• 10747+001	• 37470+002
• 41667-001	• 19936+001	• 11004+001	• 37470+002
• 41667-001	• 20000+001		• 37470+002

q = .50100+000 u = .10215+001 n = .25464+001 d1 = .11655+001 ct = .19043+001 r = .16818+004 xi = .17269+002 radius = .77130+001
 omu ALFRI ALFRI AMP ITER NSTEP
 .32100-004 19222.000 *70543-002 *10681+001 3 67
 .22000-004 14063.000 *12010+002 *14665+002 3 50

q = .50100+000 u = .10715+001 n = .25464+001 d1 = .11655+001 ct = .14026+001 r = .18841+004 xi = .17330+002 radius = .77170+001
 omu ALFRI ALFRI AMP ITER NSTEP
 .32100-004 19244.000 *70777-002 *19054+001 3 67
 .22000-004 14098.000 *12490-002 *44564+002 3 50

q = .50200+000 u = .10735+001 n = .25467+001 d1 = .11655+001 ct = .14010+001 r = .18864+004 xi = .17391+002 radius = .77210+001
 omu ALFRI ALFRI AMP ITER NSTEP
 .32100-004 19266.000 *71n1-002 *19227+001 1 63
 .22000-004 14114.000 *12970-002 *75596-002 1 50

q = .50300+000 u = .10735+001 n = .25463+001 d1 = .11655+001 ct = .13992+001 r = .18887+004 xi = .17452+002 radius = .77249+001
 omu ALFRI ALFRI AMP ITER NSTEP
 .32100-004 19289.000 *71745-002 *19400+001 1 63
 .22000-004 14138.000 *13450-002 *10776-001 1 50

q = .50400+000 u = .10235+001 n = .25463+001 d1 = .11654+001 ct = .13975+001 r = .18910+004 xi = .17513+002 radius = .77289+001
 omu ALFRI ALFRI AMP ITER NSTEP
 .32100-004 19311+000 *71979-002 *1957+001 1 63
 .22000-004 14148+000 *13930-002 *14115-001 1 50

q = .50500+000 u = .1024+001 n = .25461-002 d1 = .1335+001 ct = .1659+001 *171+001 *2546+001 *1259+001- *140+0000 *901+000
 .50500+000 1024.000 6490+000 7752+001 3452+002 1322+001 3658+001 117+001 2546+001 1251+001- 1136+000 *901+000
 .51500+000 1024.000 6490+000 7752+001 3452+002 1319+001 3658+001 111+001 2546+001 1243+001- 1133+000 *901+000
 .52500+000 1024.000 6490+000 7752+001 3452+002 1311+001 3658+001 111+001 2546+001 1235+001- 1131+000 *901+000
 .53500+000 1024.000 6490+000 7752+001 3452+002 1303+001 3658+001 111+001 2546+001 1227+001- 1129+000 *901+000
 .54500+000 1024.000 6490+000 7752+001 3452+002 1295+001 3658+001 111+001 2546+001 1219+000- 1126+000 *999+000
 .55500+000 1024.000 6490+000 7752+001 3452+002 1288+001 3658+001 117+001 2546+001 1212+001- 1125+000 *999+000
 .56500+000 1024.000 6490+000 7752+001 3452+002 1280+001 3658+001 111+001 2546+001 1204+000- 1123+000 *8886+000
 .57500+000 1024.000 6490+000 7752+001 3452+002 1273+001 3658+001 117+001 2546+001 1197+000- 1121+000 *8984+000
 .58500+000 1024.000 6490+000 7752+001 3452+002 1266+001 3658+001 111+001 2546+001 1184+000- 1120+000 *8980+000
 .59500+000 1024.000 6490+000 7752+001 3452+002 1260+001 3658+001 1170+001 2546+001 1182+000- 1119+000 *8975+000
 .60500+000 1024.000 6490+000 7752+001 3452+002 1254+001 3658+001 1170+001 2546+001 1175+001- 1117+000 *8971+000
 .61500+000 1024.000 6490+000 7752+001 3452+002 1248+001 3658+001 1170+001 2546+001 1168+000- 1116+000 *8967+000
 .62500+000 1024.000 6490+000 7752+001 3452+002 1242+001 3658+001 1170+001 2546+001 1161+001- 1107+000 *8963+000
 .63500+000 1024.000 6490+000 7752+001 3452+002 1236+001 3658+001 1170+001 2546+001 1154+001- 1103+000 *8960+000
 .64500+000 1024.000 6490+000 7752+001 3452+002 1230+001 3658+001 1170+001 2546+001 1147+001- 1098+000 *8954+000
 .65500+000 1024.000 6490+000 7752+001 3452+002 1223+001 3657+001 1170+001 2545+001 1147+001- 1098+000 *8954+000
 .66500+000 1024.000 6490+000 7752+001 3452+002 1216+001 3657+001 1170+001 2545+001 1147+001- 1095+000 *8944+000
 .67500+000 1024.000 6490+000 7752+001 3452+002 1209+001 3657+001 1170+001 2545+001 1134+001- 1077+000 *8944+000
 .68500+000 1024.000 6490+000 7752+001 3452+002 1202+001 3657+001 1170+001 2545+001 1127+001- 1078+000 *8944+000
 .69500+000 1024.000 6490+000 7752+001 3452+002 1196+001 3657+001 1170+001 2545+001 1121+001- 1097+000 *8944+000
 .70500+000 1024.000 6490+000 7752+001 3452+002 1190+001 3657+001 1170+001 2545+001 1121+001- 1097+000 *8944+000

THIS PAGE IS FAIR QUALITY PRINTED FROM COPY RECEIVED IN PDF
 41

APPENDIX B

This appendix contains an abbreviated computer printout of the restart mode for the stability analysis of the heated 9:1 ellipsoid.

DABL - FLAT PLATE UPPER SURFACE - HEATED

CONTROL PARAMETERS

```
IPL= 0  IBLTP= 0  INHAT= 1  IPOT= 0  
ISTART= 0  ITWOP= 2  IFIT= 1  IKFZ= 1  IVISC= 1  
NP= 75  IREG= 0  KF= 5
```

```
RL=      5000000.0000  ANORM= 12.000000
```

```
JMAX= 201  ETA= 6.000000  DEPS= .001000  RLDELS= .002000  
DFLS= .001000  TOL= .001000  EPS= .001000
```

INPUT BODY COORDINATES

X	Y
---	---

.00000	.00000
.20810-001	-.45100-003
.41670-001	-.13020-002
.62500-001	-.19530-002
.83330-001	-.26n40-002
.10417+000	-.32550-002
.12500+000	-.39100-002
.14543+000	-.45570-002
.16667+000	-.52080-002
.18750+000	-.58400-002
.20833+000	-.65100-002
.22917+000	-.71610-002
.25000+000	-.78125-002
.27080+000	-.84n40-002
.29167+000	-.91150-002
.31250+000	-.97660-002
.33333+000	-.10417-001
.35000+000	-.10417-001
.40000+000	-.10417-001
.50000+000	-.10417-001
.75000+000	-.10417-001
.10000+001	-.10417-001
.15000+001	-.10417-001
.20000+001	-.10417-001
.25000+001	-.10417-001
.30000+001	-.10417-001
.35000+001	-.10417-001

THIS PAGE IS A COPY OF A COPY FROM THE ORIGINAL
FROM COPY FROM THE ORIGINAL

.40000+001	-.10417-001
.45000+001	-.10417-001
.50000+001	-.10417-001
.55000+001	-.10417-001
.60000+001	-.10417-001
.65000+001	-.10417-001
.70000+001	-.10417-001
.75000+001	-.10417-001
.80000+001	-.10417-001
.85000+001	-.10417-001
.90000+001	-.10417-001
.95000+001	-.10417-001
.10000+002	-.10417-001
.10500+002	-.10417-001
.11000+002	-.10417-001
.11500+002	-.10417-001
.11750+002	-.10417-001
.11850+002	-.10417-001
.11900+002	-.10417-001
.11950+002	-.10417-001
.12000+002	.00000
.11950+002	-.10417-001
.11900+002	-.10417-001
.11850+002	-.10417-001
.11750+002	-.10417-001
.11500+002	-.10417-001
.11000+002	-.10417-001
.10500+002	-.10417-001
.10000+002	-.10417-001
.95000+001	-.10417-001
.90000+001	-.10417-001
.85000+001	-.10417-001
.75000+001	-.10417-001
.70000+001	-.10417-001
.65000+001	-.10417-001
.60000+001	-.10417-001
.55000+001	-.10417-001
.50000+001	-.10417-001
.45000+001	-.10417-001
.40000+001	-.10417-001
.35000+001	-.10417-001
.30000+001	-.10417-001
.25000+001	-.10417-001
.20000+001	-.10417-001
.15000+001	-.10417-001
.10000+001	-.10417-001
.75000+000	-.10417-001
.50000+000	-.10417-001
.40000+000	-.10417-001
.35000+000	-.10417-001
.33333+000	-.10417-001
.31250+000	.27760-002
.29167+000	.21150-002
.27080+000	.244640-002
.25000+000	.278125-002
.22917+000	.271610-002

+20811+000	.65100-002
+11750+000	.58600-002
+16647+000	.52680-002
+14583+000	.45570-002
+12500+000	.39100-002
+10417+000	.32650-002
+81110-001	.26140-002
+62500-001	.19530-002
+41570-001	.13n20-002
+20810-001	.65100-003
.00000	.00000

BODY BOUNDARY LAYER - HEATED

ITTE= 1 TTEMP1= 23.89000 DTTEMP= 2.78000 ITTEMP1= 1 ITTEMP2= 95

POTENTIAL FLOW SOLUTION AND TEMPERATURE DISTRIBUTION
Y=X/ANORM, Y=Y/ANORM

X	Y	S	U	T
.00000	.00000			.26670*002
.17358-002	.54250-004	.86834-003	.47480+000	.26670*002
.34725-002	.10850-003	.26054-002	.97240+000	.26670*002
.52083-002	.14275-003	.43425-002	.97929+000	.26670*002
.69442-002	.21700-003	.60792-002	.98395+000	.26670*002
.86806-002	.27125-003	.78162-002	.98754+000	.26670*002
.10417-001	.32503-003	.95533-002	.99071+000	.26670*002
.12152-001	.37975-003	.11290-001	.99337+000	.26670*002
.13889-001	.43400-003	.13027-001	.99566+000	.26670*002
.15625-001	.48833-003	.14764-001	.99805+000	.26670*002
.17361-001	.54250-003	.16501-001	.10001+001	.26670*002
.19098-001	.59675-003	.18238-001	.10026+001	.26670*002
.20813-001	.65104-003	.19975-001	.10048+001	.26670*002
.22567-001	.70531-003	.21711-001	.10071+001	.26670*002
		.21448-001	.10092+001	

THIS PAGE IS THE LAST ONE OF THE DOCUMENT
AND WAS RECEIVED BY US

.24306-001	.75958-003			
.26042-001	.81383-003	.25186-001	.10087+001	.26670+002
.27777-001	.86808-003	.26723-001	.99030+000	.26670+002
.22167-001	.86808-003	.28486-001	.98659+000	.26670+002
.13333-001	.86808-003	.31264-001	.10057+001	.26670+002
.11667-001	.86808-003	.37514-001	.10092+001	.26670+002
.62500-001	.86808-003	.52097-001	.10154+001	.26670+002
.73333-001	.86808-003	.72230-001	.10034+001	.26670+002
.12500+000	.86808-003	.10418+000	.10055+001	.26670+002
.16667+000	.86808-003	.14585+000	.10027+001	.26670+002
.20833+000	.86808-003	.18751+000	.10017+001	.26670+002
.25000+000	.86808-003	.22918+000	.10014+001	.26670+002
.29167+000	.86808-003	.27085+000	.10013+001	.26670+002
.33333+000	.86808-003	.31251+000	.10012+001	.26670+002
.37500+000	.86808-003	.35418+000	.10011+001	.26670+002
.41667+000	.86808-003	.39585+000	.10011+001	.26670+002
.45833+000	.86808-003	.43751+000	.10011+001	.26670+002
.50000+000	.86808-003	.47918+000	.10011+001	.26670+002
.54167+000	.86808-003	.52085+000	.10011+001	.26670+002
.58333+000	.86808-003	.56251+000	.10011+001	.26670+002
.62500+000	.86808-003	.60418+000	.10012+001	.26670+002
.66667+000	.86808-003	.64585+000	.10012+001	.26670+002
.70833+000	.86808-003	.68751+000	.10013+001	.26670+002
.75000+000	.86808-003	.72918+000	.10015+001	.26670+002
.79167+000	.86808-003	.77085+000	.10015+001	.26670+002
.83333+000	.86808-003	.81251+000	.10019+001	.26670+002
.87500+000	.86808-003	.85418+000	.10024+001	.26670+002
.91667+000	.86808-003	.89585+000	.10037+001	.26670+002
.95833+000	.86808-003	.93751+000	.10070+001	.26670+002

THIS PAGE IS BEST QUALITY PRACTICABLE
FROM COPY EXISTING TO BDC

START AUNIARY LAYER/STABILITY ANALYSIS

S	UFF	DUF	RADIUS	BETA	GAAMA	DELTA	DI	H	C1	CQ	VISCR
.4000-002	.9812+000	.10442+000	.1000+001	.24222-008	.6076+002	.3460+001	.1047+001	.12491+001	.6512+005	.2819+004	.9421+000
.4000-003	.98135+000	.10078+001	.1000+001	.24222+002	.3529+001	.1135+001	.1259+001	.1473+002	.703+000	.9421+000	.9421+000
.400750+003	.98090+003	.10032+001	.1000+001	.24670+002	.3529+001	.1137+001	.1250+001	.1098+002	.5265+000	.9421+000	.9421+000
.779167+000	.98090+003	.10032+001	.1000+001	.24670+002	.3529+001	.1137+001	.1250+001	.1098+002	.5265+000	.9421+000	.9421+000
.779167+000	.98090+003	.10032+001	.1000+001	.24670+002	.3529+001	.1137+001	.1250+001	.1098+002	.5265+000	.9421+000	.9421+000
.99543+000	.98090+003	.10032+001	.1000+001	.24670+002	.3529+001	.1137+001	.1250+001	.1098+002	.5265+000	.9421+000	.9421+000
.99543+000	.98090+003	.10032+001	.1000+001	.24670+002	.3529+001	.1137+001	.1250+001	.1098+002	.5265+000	.9421+000	.9421+000
.10000+001	.00000	.00000	.0000+001	.266670+002	.3563+001	.1148+001	.1264+001	.1467+001	.1285+000	.9421+000	.9421+000
.10000+001	.00000	.00000	.0000+001	.266670+002	.3563+001	.1148+001	.1264+001	.1467+001	.1285+000	.9421+000	.9421+000
.12000-001	.9916+000	.1739+000	.1000+001	.1307+001	.1572+002	.1574+001	.1146+001	.1135+001	.1473+002	.703+000	.9421+000
.12000-001	.9916+000	.1739+000	.1000+001	.1307+001	.1572+002	.1574+001	.1146+001	.1135+001	.1473+002	.703+000	.9421+000
.14000-001	.9913+000	.1307+001	.1000+001	.1307+001	.1572+002	.1574+001	.1146+001	.1135+001	.1473+002	.703+000	.9421+000
.14000-001	.9913+000	.1307+001	.1000+001	.1307+001	.1572+002	.1574+001	.1146+001	.1135+001	.1473+002	.703+000	.9421+000
.16000-001	.9910+000	.1304+001	.1000+001	.2210+000	.7918+001	.3609+001	.1148+001	.1253+001	.7764+001	.3194+000	.9421+000
.16000-001	.9910+000	.1304+001	.1000+001	.2210+000	.7918+001	.3609+001	.1148+001	.1253+001	.7764+001	.3194+000	.9421+000
.18000-001	.9902+001	.1266+001	.1000+001	.3007+001	.6470+001	.3612+001	.1148+001	.1254+001	.6967+001	.3155+000	.9421+000
.18000-001	.9902+001	.1266+001	.1000+001	.3007+001	.6470+001	.3612+001	.1148+001	.1254+001	.6967+001	.3155+000	.9421+000
.20000-001	.9905+001	.1408+001	.1000+001	.3889+001	.6020+001	.3610+001	.1149+001	.1253+001	.6042+001	.2664+000	.9421+000
.22000-001	.1007+001	.912+000	.1000+001	.2483+001	.5641+001	.3610+001	.1140+001	.1253+001	.5683+001	.2662+000	.9421+000
.24000-001	.1010+001	.1850+000	.1000+001	.6508+001	.5331+001	.3602+001	.1132+001	.1251+001	.5545+001	.2555+000	.9421+000
.24000-001	.1010+001	.1850+000	.1000+001	.6508+001	.5331+001	.3602+001	.1132+001	.1251+001	.5545+001	.2555+000	.9421+000
.26000-001	.9958+002	.1825+001	.1000+001	.1726+002	.4701+001	.3507+001	.1037+001	.9236+001	.7050+001	.2434+000	.9421+000
.26000-001	.9958+002	.1825+001	.1000+001	.1726+002	.4701+001	.3507+001	.1037+001	.9236+001	.7050+001	.2434+000	.9421+000
.30000-001	.9919+000	.1005+001	.1000+001	.3059+000	.4551+001	.3181+001	.1038+001	.9210+001	.5560+001	.2194+000	.9421+000
.32000-001	.1010+001	.4433+001	.1000+001	.2557+000	.4433+001	.3431+001	.1022+001	.9238+001	.6072+001	.2192+000	.9421+000
.34000-001	.1014+001	.1456+000	.1000+001	.7969+002	.4287+001	.3163+001	.1025+001	.9229+001	.5029+001	.204+000	.9421+000
.36000-001	.1012+001	.1012+001	.1000+001	.1036+000	.4131+001	.3476+001	.1038+001	.9244+001	.4926+001	.2081+000	.9421+000
.38000-001	.1008+001	.1381+001	.1000+001	.6720+000	.3985+001	.3479+001	.1042+001	.9249+001	.4669+001	.1958+000	.9421+000
.40000-001	.0077+001	.4494+000	.1000+001	.3154+001	.3855+001	.3493+001	.1055+001	.9342+001	.4167+000	.9421+000	.9421+000
.42000-001	.1006+001	.2306+001	.1000+001	.1499+001	.3748+001	.3519+001	.1071+001	.9428+001	.4028+001	.1796+000	.9421+000
.44000-001	.1007+001	.7901+000	.1000+001	.5551+001	.3651+001	.3512+001	.1074+001	.9429+001	.4003+001	.1762+000	.9421+000
.46000-001	.1009+001	.1005+001	.1000+001	.8141+001	.3565+001	.3510+001	.1072+001	.9465+001	.3495+001	.1727+000	.9421+000

STABILITY AUTO START SEARCH FOR RC

S+	0.00000	RC+	R0+	R0+	R0+	R0+	R0+	R0+	R0+	R0+	R0+
S+	-0.00000	RC+	7.44+042	R0+	5.96+081	R0+	6.73+228	R0+	6.86+923	R0+	159.790
S+	-0.01290	RC+	7.44+042	R0+	7.07+556	R0+	7.64+325	R0+	7.67+713	R0+	225.907
S+	-0.01400	RC+	7.44+042	R0+	7.15+601	R0+	7.75+556	R0+	8.43+556	R0+	270.620
S+	-0.01460	RC+	7.44+042	R0+	7.23+647	R0+	8.01+594	R0+	8.61+609	R0+	327.145
S+	-0.01460	RC+	7.44+042	R0+	7.23+647	R0+	8.01+594	R0+	8.61+609	R0+	361.609
S+	-0.01460	RC+	7.44+042	R0+	7.23+647	R0+	8.01+594	R0+	8.61+609	R0+	395.195
S+	-0.02200	RC+	7.44+042	R0+	7.57+713	R0+	8.45+124	R0+	9.25+753	R0+	455.124
S+	-0.02400	RC+	7.44+042	R0+	7.81+737	R0+	9.01+594	R0+	9.83+505	R0+	513.505
S+	-0.07400	RC+	7.44+042	R0+	2.01+155	R0+	1.072+001	R0+	1.3975+001	R0+	1.727+000

THIS PAGE IS BEST QUALITY PRACTICALLY
FROM COPY FROM THE TUTORIAL

S	U	F	R	FF	HUR	RADIUS	BETA	GAMMA	DELTA	DELIN	D1	H	CY	CQ	VISCR
S#	02400	Rc=	3709.964	RD=	446.001										
S#	03050	Rc=	3378.383	RD=	500.101										
S#	03200	Rc=	03954.582	RD=	503.404										
S#	03400	Rc=	1781.434	RD=	541.941										
S#	03600	Rc=	1062.185	RD=	568.476										
S#	03800	Rc=	1575.911	RD=	549.382										
S#	04000	Rc=	1122.042	RD=	615.245										
S#	04200	Rc=	087.187	RD=	642.906										
S#	04400	Rc=	854.474	RD=	662.593										
S#	04600	Rc=	755.428	RD=	678.528										
S#	04700-001	+1009+001	+1035+001	+1000+001	+8.41+001	+3565+001	+3493+001	+1072+001	+2486+001	+3990+001	+1135+000	+9421+000			
S#	04800-001	+1011+001	+1122+001	+1000+001	+9.23+001	+9.23+001	+3489+001	+2477+001	+1069+001	+2477+001	+1705+000	+9421+000			
S#	04900-001	+1014+001	+1035+001	+1000+001	+3.42+001	+3.42+001	+3489+001	+1069+001	+2477+001	+2894+001	+1667+000	+9421+000			
S#	05000-001	+1015+001	+6765+000	+1000+001	+6.05+001	+3.34+001	+3492+001	+1071+001	+2481+001	+3774+001	+1627+000	+9421+000			
S#	05100-001	+1016+001	+2646+000	+1000+001	+2.46+001	+3.27+001	+3502+001	+1081+001	+2496+001	+3571+001	+1577+000	+9421+000			
S#	05200-001	+1016+001	+9076+000	+1000+001	+8.65+002	+2.72+001	+3513+001	+1071+001	+2510+001	+3481+001	+1535+000	+9421+000			
S#	05300-001	+1016+001	+3849+000	+1000+001	+3.14+001	+3.14+001	+3518+001	+1094+000	+2512+001	+3456+001	+1505+000	+9421+000			
S#	05400-001	+1015+001	+6206+000	+1000+001	+6.51+001	+3.08+001	+3516+001	+1092+000	+2504+000	+3463+001	+1485+000	+9421+000			
S#	05500-001	+1013+001	+7911+000	+1000+001	+8.79+001	+2.02+001	+3512+001	+1097+001	+2495+001	+3451+001	+1464+000	+9421+000			
S#	05600-001	+1013+001	+9147+000	+1000+001	+1.01+002	+2.02+001	+3506+001	+1082+000	+2486+001	+3451+001	+1449+000	+9421+000			
S#	05700-001	+1010+001	+9776+000	+1000+001	+1.15+001	+2.90+001	+3500+001	+1076+001	+2476+001	+3436+001	+1123+000	+9421+000			
S#	05800-001	+1008+001	+9777+000	+1000+001	+1.19+000	+2.85+001	+3495+001	+1072+001	+2466+001	+3298+001	+1101+000	+9421+000			
S#	05900-001	+1006+001	+9214+000	+1000+001	+1.16+000	+2.80+001	+3492+001	+1069+001	+2455+001	+3242+001	+1128+000	+9421+000			
S#	06000-001	+1004+001	+7924+000	+1000+001	+1.04+001	+2.75+000	+3491+001	+1068+001	+2466+001	+3176+001	+1153+000	+9421+000			
S#	06100-001	+1003+001	+6266+000	+1000+001	+8.49+001	+2.71+001	+3492+001	+1069+001	+2469+001	+3082+001	+1126+000	+9421+000			
S#	06200-001	+1002+000	+4635+000	+1000+001	+1.00+002	+2.62+001	+3493+001	+1073+001	+2475+001	+2988+001	+1103+000	+9421+000			
S#	06300-001	+1001+001	+3171+000	+1000+001	+1.15+001	+2.60+001	+3502+001	+1076+001	+2468+001	+2864+001	+1127+000	+9421+000			
S#	06400-001	+1001+001	+1854+000	+1000+001	+1.04+001	+2.25+001	+3507+001	+1084+001	+2479+001	+2790+001	+1129+000	+9421+000			
S#	06500-001	+1000+001	+3375+001	+1000+001	+5.29+002	+2.52+001	+3521+001	+1097+001	+2510+001	+2692+001	+1129+000	+9421+000			
S#	06600-001	+1000+001	+1213+000	+1000+001	+1.14+001	+2.49+001	+3527+001	+1101+001	+2517+001	+2583+001	+1146+000	+9421+000			

STABILITY AUTO START SEARCH FOR RC

S=	*044600	RC=	747-695	RD=	675-459
S=	*048009	RC=	1118-853	RD=	689-872
S=	*052000	RC=	1212-506	RD=	705-703
S=	*052000	RC=	1161-652	RD=	724-251
S=	*054000	RC=	985-791	RD=	796-379
S=	*054000	RC=	816-312	RD=	768-771
S=	*058000	RC=	773-979	RD=	787-126
PC=	0MF6C=	773-979	RD=	787-128	ALPIAC=
	0MF6C=	000011299	SD=	005000	

1987 10-10-10
WATER 1000 ml

$\zeta = .11268-003$ $U = .21221+000$ $H = .13937-002$ $\alpha = .00000$ $\beta = .00000$ $\gamma = .5$ $\delta = .47$
 $.91693-004$ $.2035+000$ $.37063-002$ $.00000$ $.00000$ $.6$ $.48$
 $.77765-004$ $.17008+000$ $.67283-002$ $.00000$ $.00000$ $.6$ $.43$
 $.64545-004$ $.15342+000$ $.98288-002$ $.00000$ $.00000$ $.6$ $.39$
 $.51573-004$ $.13243+000$ $.17600-001$ $.00000$ $.00000$ $.6$ $.37$

$\zeta = .60700-001$ $U = .10149+001$ $H = .25031+001$ $D1 = .10081+001$ $D2 = .10081+001$ $CT = .35627+001$ $R = .79410+003$ $X1 = .53263-001$ $RADIUS = .10000+001$
 $O(H)$ $A(LFRI)$ $A(LFIU)$ $A(MP)$ $ITER$ $NSTEP$
 $.11268-003$ $.21377+000$ $.13780-002$ $.00000$ 4 47
 $.93693-004$ $.20457+000$ $.35450-002$ $.00000$ $.00000$ 4 42
 $.77765-004$ $.17912+000$ $.65035-002$ $.00000$ $.00000$ 4 40
 $.64545-004$ $.15422+000$ $.95971-002$ $.00000$ $.00000$ 3 36
 $.51573-004$ $.13307+000$ $.12368-001$ $.00000$ $.00000$ 3 32

$\zeta = .60700-001$ $U = .10149+001$ $H = .25031+001$ $D1 = .10085+001$ $D2 = .10085+001$ $CT = .35669+001$ $R = .80145+003$ $X1 = .54481-001$ $RADIUS = .10000+001$
 $O(H)$ $A(LFRI)$ $A(LFIU)$ $A(MP)$ $ITER$ $NSTEP$
 $.11268-003$ $.29530+000$ $.16715-002$ $.00000$ 3 47
 $.93693-004$ $.20960+000$ $.36764-002$ $.00000$ $.00000$ 3 43
 $.77765-004$ $.16009+000$ $.64933-002$ $.00000$ $.00000$ 3 40
 $.64545-004$ $.15503+000$ $.94775-002$ $.00000$ $.00000$ 3 37
 $.51573-004$ $.13371+000$ $.12259-001$ $.00000$ $.00000$ 3 33

$\zeta = .61640-001$ $U = .10138+001$ $H = .24964+001$ $D1 = .10027+001$ $D2 = .10027+001$ $CT = .35596+001$ $R = .80981+003$ $X1 = .55942-001$ $RADIUS = .10000+001$
 $O(H)$ $A(LFRI)$ $A(LFIU)$ $A(MP)$ $ITER$ $NSTEP$
 $.11268-003$ $.29733+000$ $.23144-002$ $.00000$ 3 46
 $.93693-004$ $.21172+000$ $.30128-002$ $.00000$ $.00000$ 3 43
 $.77765-004$ $.18134+000$ $.66679-002$ $.00000$ $.00000$ 3 40
 $.64545-004$ $.15603+000$ $.95704-002$ $.00000$ $.00000$ 3 37
 $.51573-004$ $.13452+000$ $.12278-001$ $.00000$ $.00000$ 3 34

$\zeta = .61368-001$ $U = .10121+001$ $H = .24875+001$ $D1 = .10078+001$ $D2 = .10078+001$ $CT = .35585+001$ $R = .81879+003$ $X1 = .57692-001$ $RADIUS = .10000+001$
 $O(H)$ $A(LFRI)$ $A(LFIU)$ $A(MP)$ $ITER$ $NSTEP$
 $.11268-003$ $.29777+000$ $.32698-002$ $.00000$ 3 46
 $.93693-004$ $.21136+000$ $.45902-002$ $.00000$ $.00000$ 3 43
 $.77765-004$ $.18849+000$ $.70449-002$ $.00000$ $.00000$ 3 39
 $.64545-004$ $.15722+000$ $.98179-002$ $.00000$ $.00000$ 3 36
 $.51573-004$ $.13144+000$ $.17444-001$ $.00000$ $.00000$ 3 34

THIS PAGE IS BEST QUALITY PRACTICABLE
FROM COPY FURNISHED TO BDC